Plasmonic Enhancement of Graphene Heterostructure based Terahertz Detectors

Vladimir Mitin

University at Buffalo, Buffalo, NY 14260

The work was done in collaboration with:

Victor Ryzhii

Taiichi Otsuji

Vladimir Aleshkin

Alexander Dubinov

Maxim Ryzhii

Michael Shur

Outline

- Introduction and Motivation
- Optoelectronic Properties of Graphene
- Optically Pumped THz Lasers
- Current Injection THz Lasers
- Double Graphene Layer Structures
- Plasmonic Enhancement
- Summary

Outline

- *Introduction and Motivation*
- Optoelectronic Properties of Graphene
- Optically Pumped THz Lasers
- Current Injection THz Lasers
- Double Graphene Layer Structures
- Plasmonic Enhancement
- Summary

Carbon structures (carbon allotropies). What is graphene?

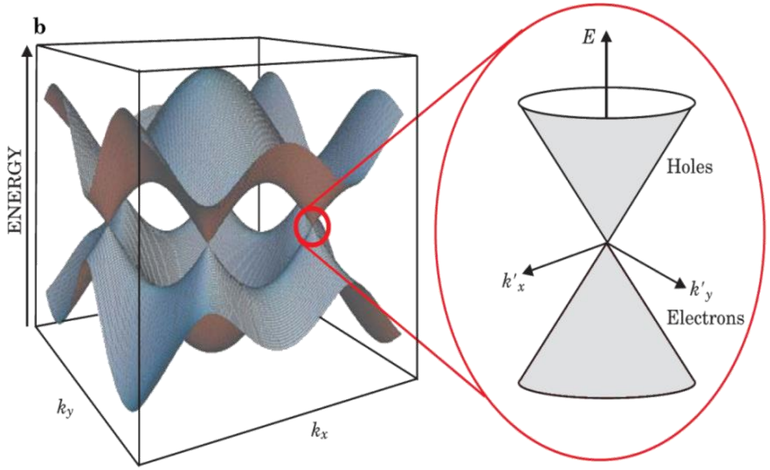

Graphene gapless band structure

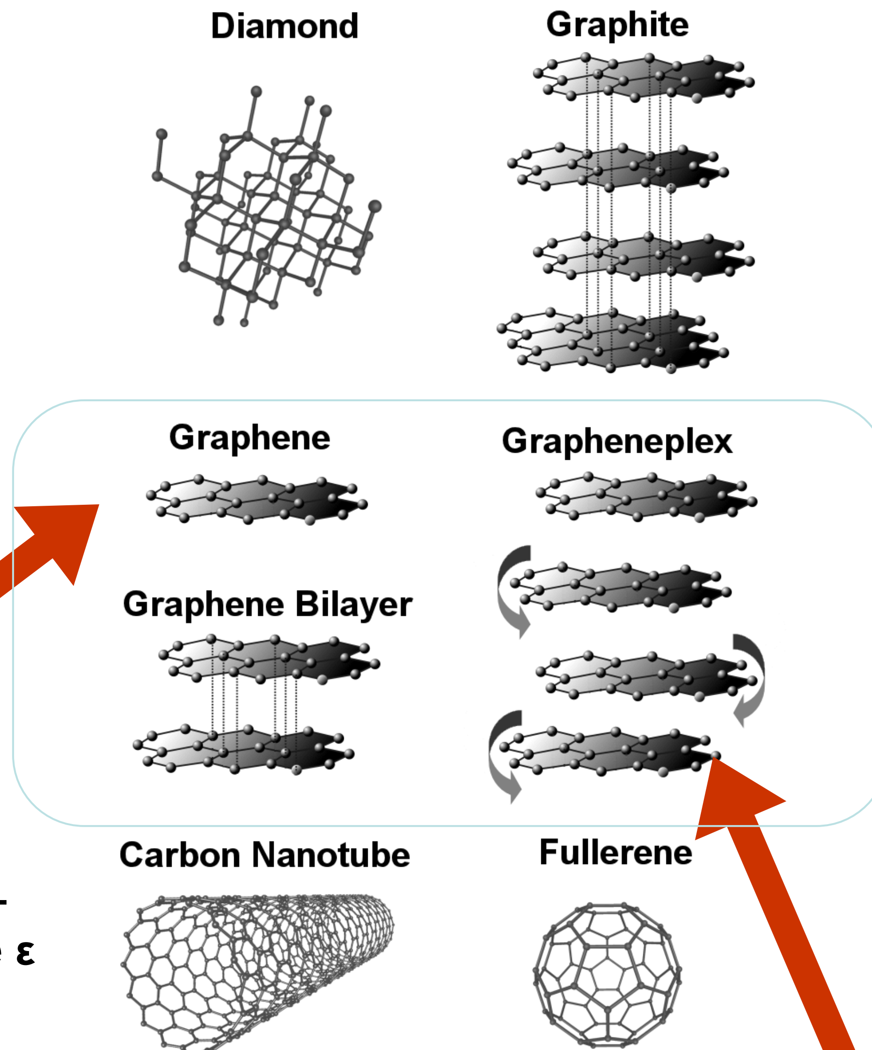

Graphene **– a dense honeycomb monolayer of carbon atoms forming two-dimensional crystal structure.**

Gapless energy spectrum **of graphene – a linear dependence of electron and hole ε on momentum absolute value p ($\varepsilon = \pm v_F\, p$, where $v_F \approx 10^8$ cm/s).**

Multiple disoriented non-Bernal stacked graphene Layer structure – Absolutely New Material for Optoelectronics!!!

Synthesis of Graphene

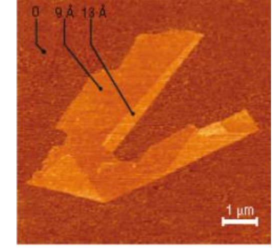

- **Peeling from HOPG (highly oriented pyrolytic graphite)**
  - Highest mobility obtained
  - Reproducibility is challenging

  A. Geim and K. Novoselov, ***Nat. Mat. 6****, 184 (2007).*

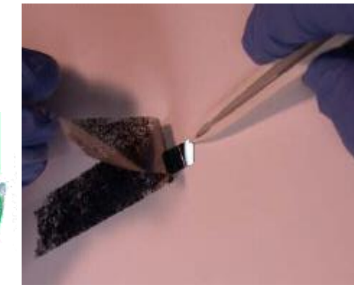

- **Epitaxial graphene: thermal decomposition of hexagonal SiC**
  - Process temperature rather high ~1000
  - Better mobility than CVD growth

  W.A. de Heer et al., ***Solid State Commun. 143****, 92 (2007).*
  M. Suemitsu and H. Fukidome, ***J. Phys. D 43****, 374012 (2010).*

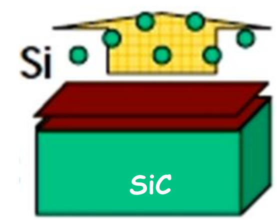

- **CVD growth on metallic catalyst and transferring substrate**
  - Cu, Ni, Fe, Co etc.. at low temperature 650 – 1000 ℃
  - Large area, quality being improved
  - Epitaxial CVD graphene now available
  - Transfer process mandatory

  J. Bae et al, ***Nature Nanotech. 5****, 574 (2010).*
  H. Ago et al., ***ACS Nano 4****, 7404 (2010).*

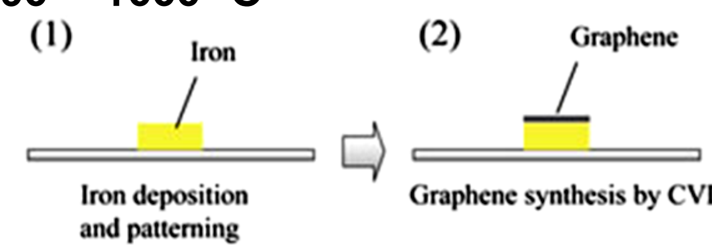

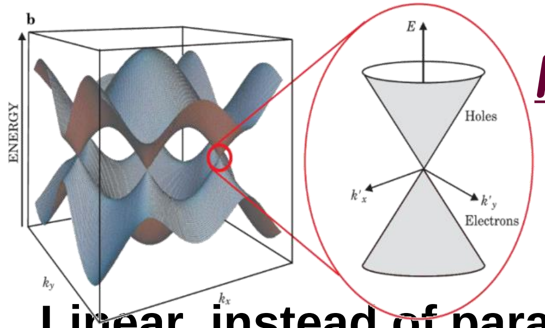

Features of graphene and their consequences

Frequency multiplication devices

- Linear, instead of parabolic, dispersion relation for electron holes leads to new nonlinear properties

THz/IR detectors and sources

- Zero energy gap allows absorption and emission of low energy photons (absorption coefficient = 0.023) and effective interband tunneling

High-speed transistors and plasma-wave THz devices

- High electron (hole) mobility (up to <u>200,000 cm^2/V s</u> at T = 300K) and high electron and hole velocities (10^8 cm/s) - ballistic transport in micrometer scale

Transistor and optoelectronic devices optimization

- Band-gap engineering in nanoribbon and bilayer structures

Voltage tunability of device characteristics

- Effective voltage control – inversion of carrier type, electrically induced p-n-junctions

Novel MEMS/NEMS

- Exceptional mechanical properties

Interconnections

- Large current density

?

Why graphene attracted attention of researchers?

?

Why graphene attracted attention of researchers?

($\varepsilon = \pm v_F\, p$, where $v_F \approx 10^8$ cm/s).

Zero Band gap

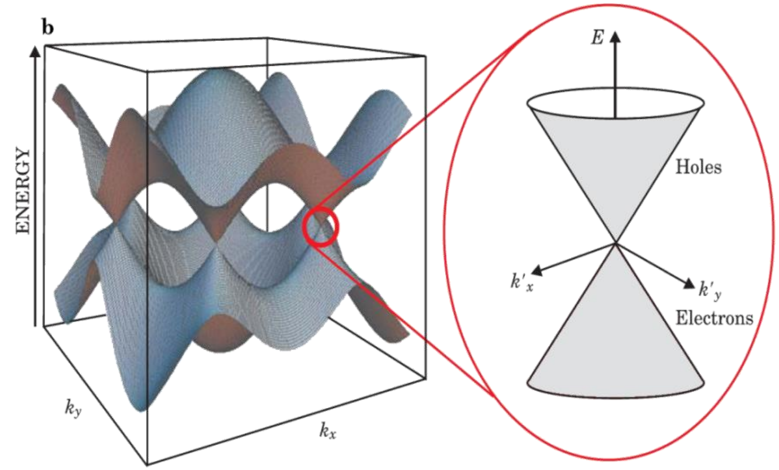

Linear (rather than quadratic) dispersion

Just a nonolayer thick material

Outline

- Introduction and Motivation
- *Optoelectronic Properties of Graphene*
- Optically Pumped THz Lasers
- Current Injection THz Lasers
- Double Graphene Layer Structures
- Plasmonic Enhancement
- Summary

Ultra-Broadband Flat Optical Response Due to Gapless/Linear Energy Spectra

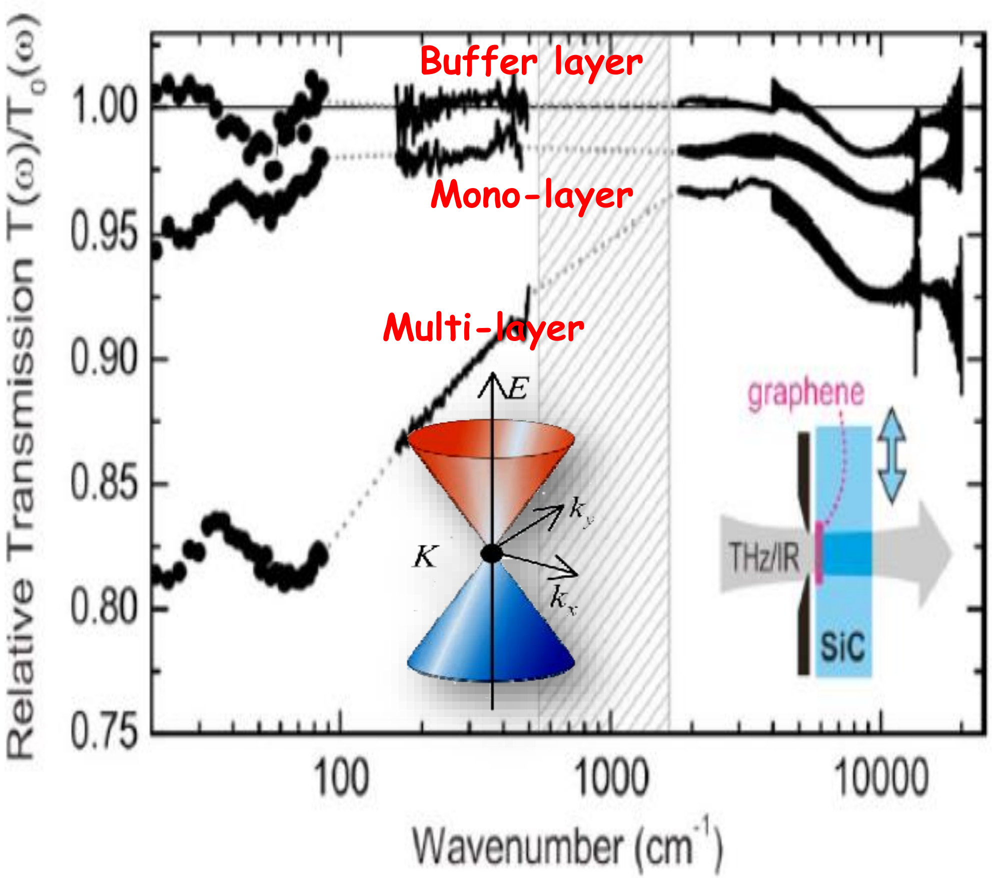

H. Choi et al., ***APL 94***, *172102 (2009).*

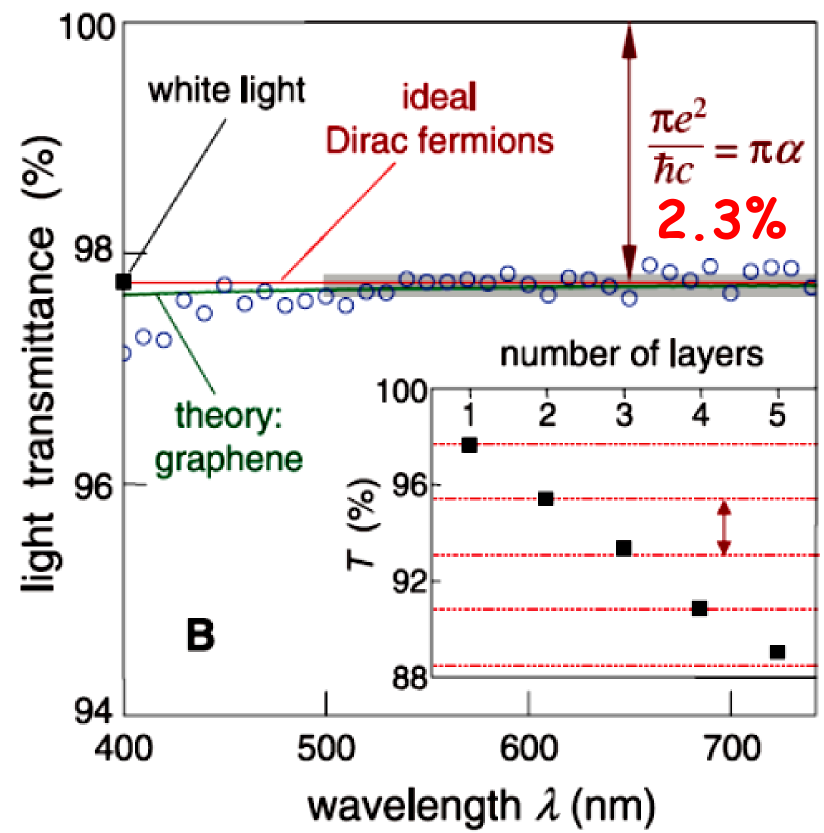

R.R. Nair et al., ***Science 320***, *1308 (2008).*

Bandgap Engineering for Graphene

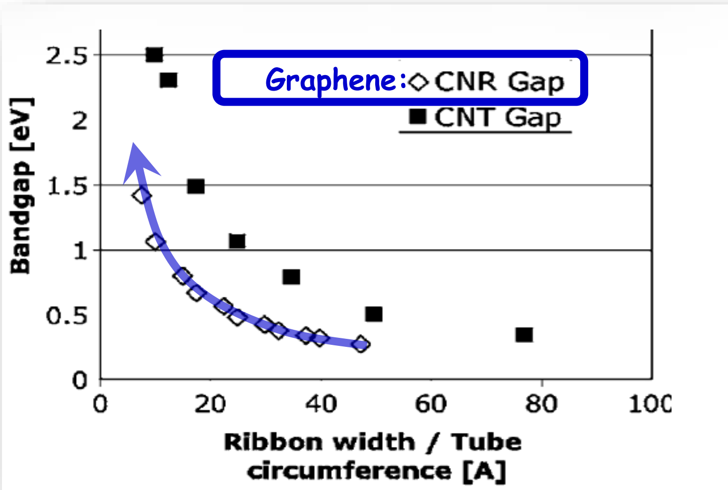

B. Obradovic et al., ***APL 88***, 142102(2006).

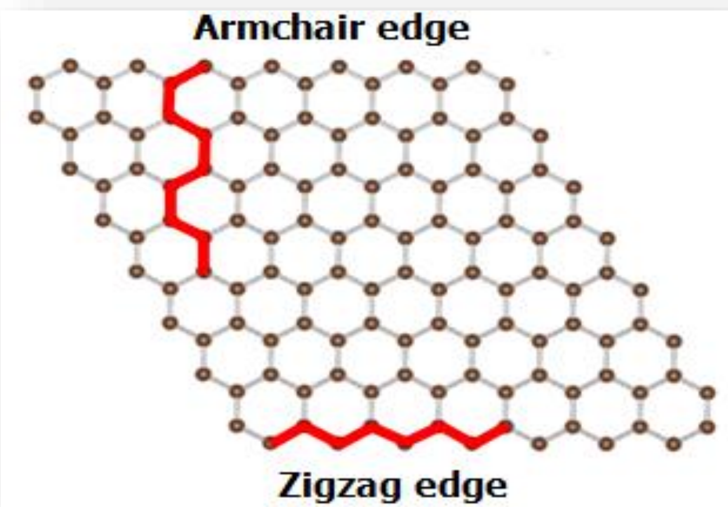

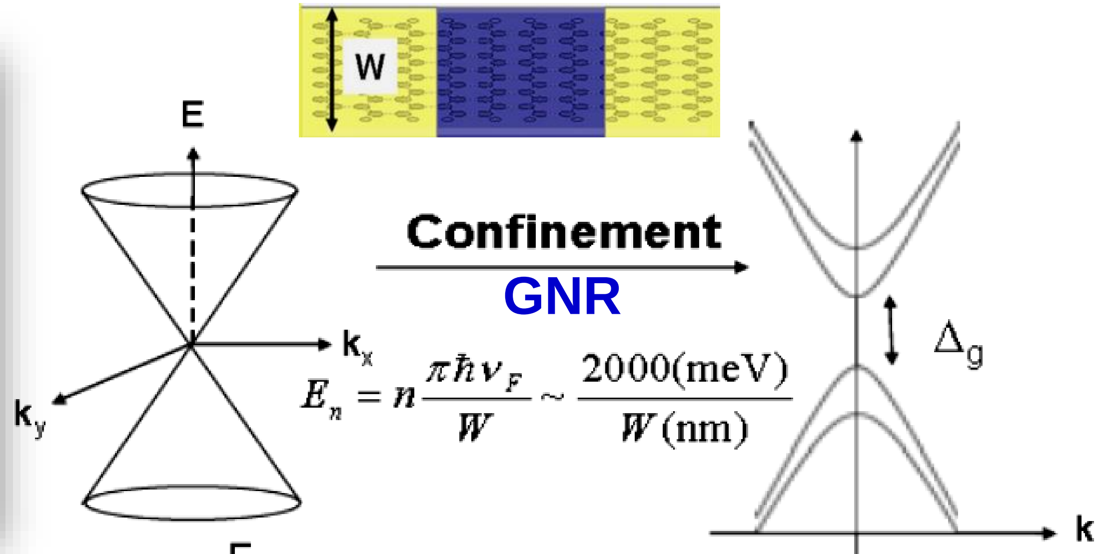

$$E_n = n\frac{\pi\hbar v_F}{W} \sim \frac{2000(\text{meV})}{W(\text{nm})}$$

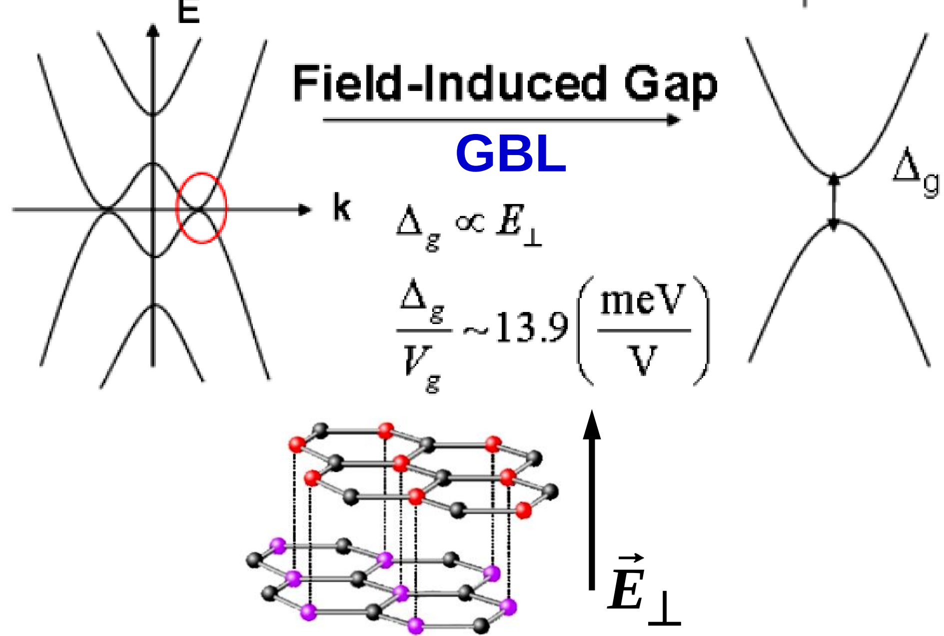

$$\Delta_g \propto E_\perp$$

$$\frac{\Delta_g}{V_g} \sim 13.9\left(\frac{\text{meV}}{\text{V}}\right)$$

?

Does absorphion coefficient of graphene depend on frequency?

?

Does absorphion coefficient of graphene depend on frequency?

No, it is frequency independent

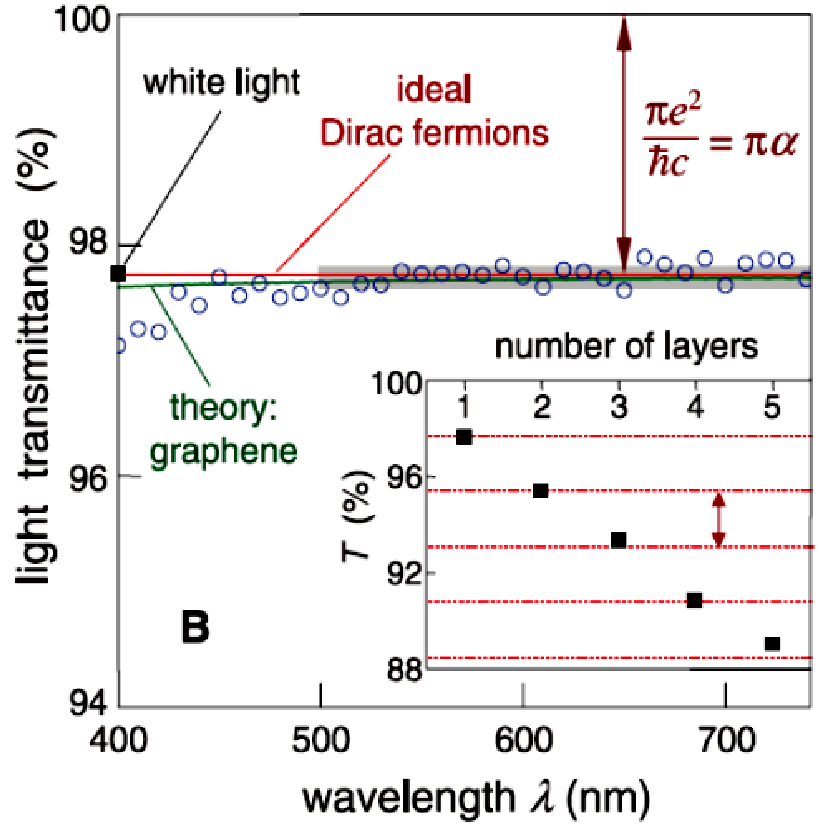

Outline

- Introduction and Motivation
- Optoelectronic Properties of Graphene
- *Optically Pumped THz Lasers*
- Current Injection THz Lasers
- Double Graphene Layer Structures
- Plasmonic Enhancement
- Summary

Carrier Relaxation Dynamics after Optical Pumping and Population Inversion at RT

Major carrier scatterings

Intraband optical-phonon (OP) scattering	⇨	**Energy relaxation (100 fs ~ 1 ps)**
Interband OP scattering	⇨	**Energy relaxation & Recombination (1~10 ps)**
Carrier-carrier (CC) scattering	⇨	**Quasi-equilibration (10~100 fs)**

Distribution function

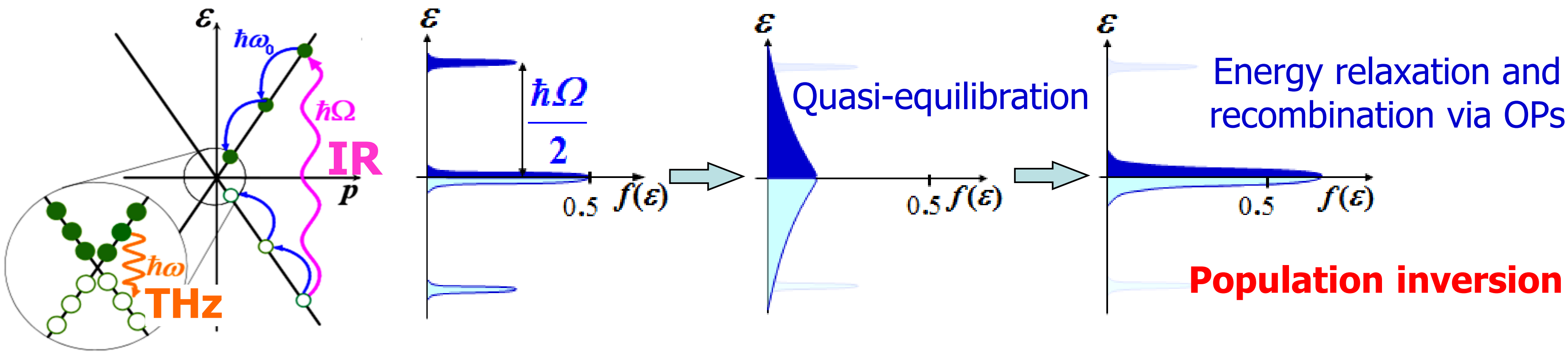

Experiments suggest CC scattering is dominant at room temperature and/or strong excitation.

D. Sun et al., ***PRL 101***, *157402 (**2008**).*
P.A. George et al., ***Nano Lett. 8***, *4248 (**2008**).*
J. Dawlaty et al., ***APL 92***, *042116 (**2008**).*
M. Breusing et al., ***PRL 102***, *086809 (**2009**).*

Observation of Threshold Behavior, Proving Stimulated THz Emission & Gain

Details with new data TBP at W4B.3 16:00~

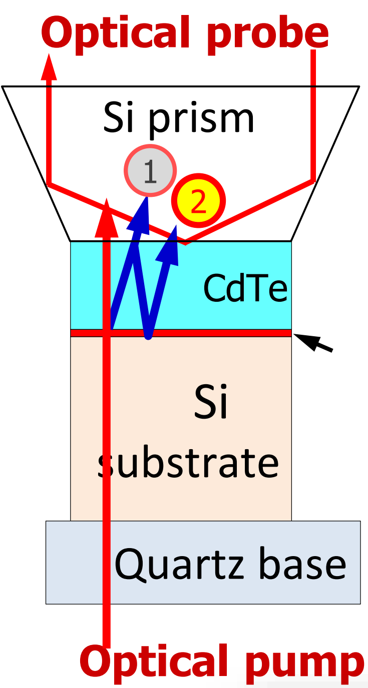

Experimental result

S. Boubanga Tombet et al., ***arXiv****:1011.2618 (2011).*

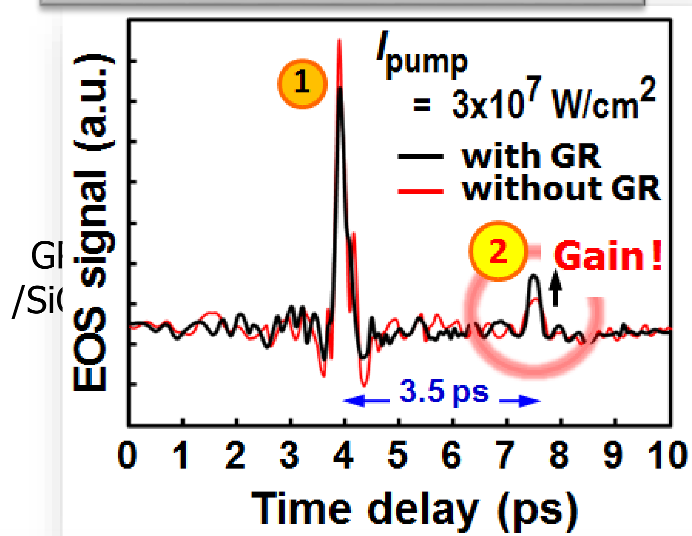

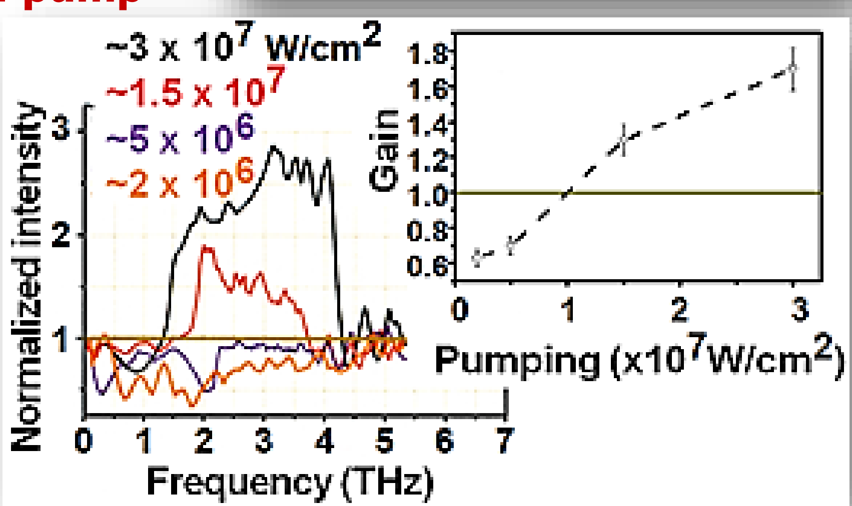

Theoretical result

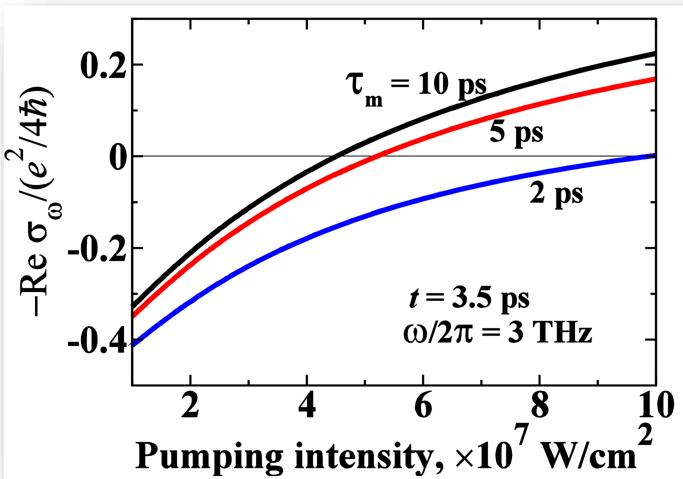

- **Qualitative agreement of threshold behavior !**
- **Possible reason for quantitative difference: CC scattering not so dominant.**

What is the Minimum Lasing Frequency?

Effect of quality

Decrease in maximum gain; shift toward higher frequencies dependences!!!

Slot vs. dielectric waveguide

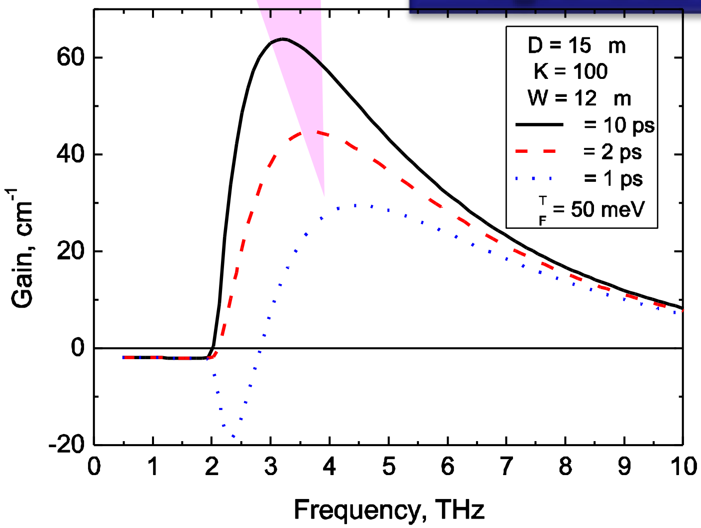

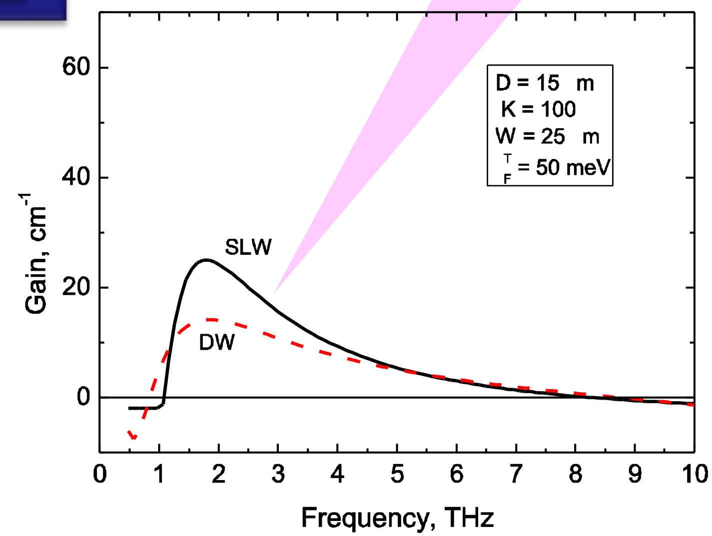

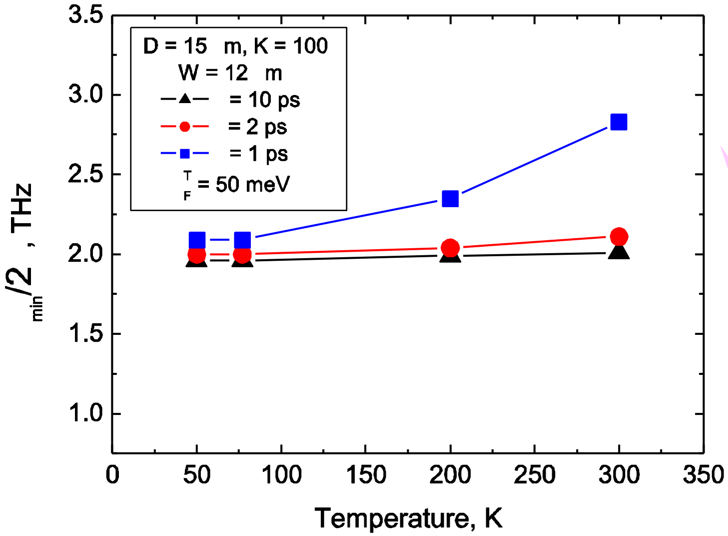

Minimum frequency vs. temperature

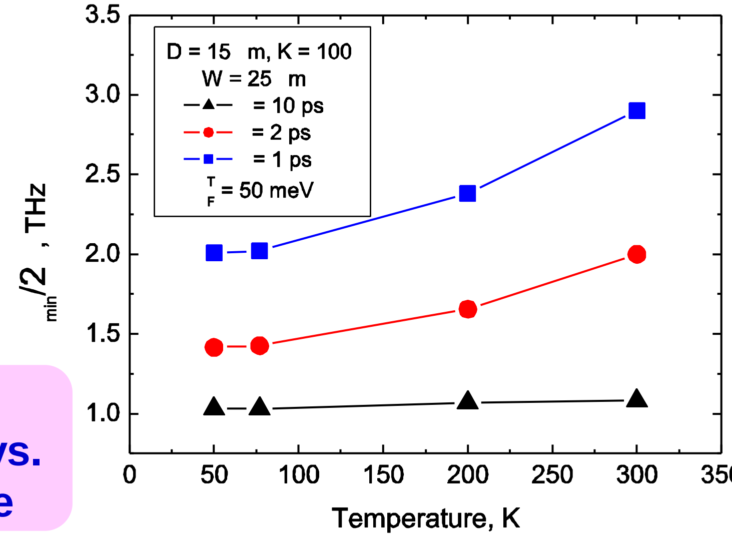

Hindering effects on stimulated emission mechanism

- ***Recombination Processes***

  Population inversion is suppressed in the active region, for energies $>\hbar\omega_0/2$, while recombination is weak in the passive region, $<\hbar\omega_0$

- ***Long-Range Disorder***

  Separation of e-h pairs due to random potential increases the averaged min concentration for the population inversion condition

- ***Small Active Volume***

  Since ~3 A thickness of graphene, active volume (and an output power) can be increased using large-area (or long) samples

- ***Losses in Resonator***

  Losses of metal (or heavily-doped) resonators in QCL ~50 cm^{-1}; a dielectric waveguide (e.g. Si-fiber) can be used as resonator

Methods of e-h pairs excitation

- ***Electrical injection through pn-junction***
- ***Optical pumping with lateral diffusion***
- ***Pulse optical excitation***

Outline

- Introduction and Motivation
- Optoelectronic Properties of Graphene
- Optically Pumped THz Lasers
- *Current Injection THz Lasers*
- Double Graphene Layer Structures
- Plasmonic Enhancement
- Summary

Toward the Creation of Graphene Current-Injection THz Lasers

*M. Ryzhii and V. Ryzhii, **JJAP 46**, L151 (2007).*
*V. Ryzhii, M. Ryzhii, V. Mitin, and T. Otsuji, **JAP**, in press.*

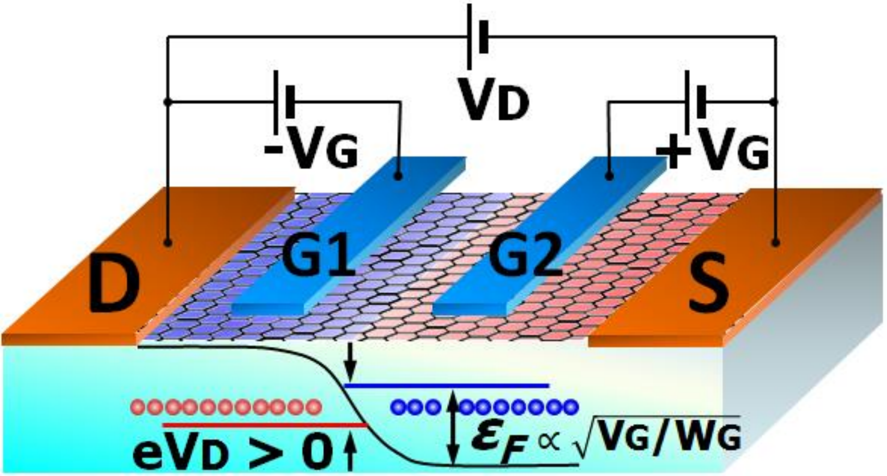

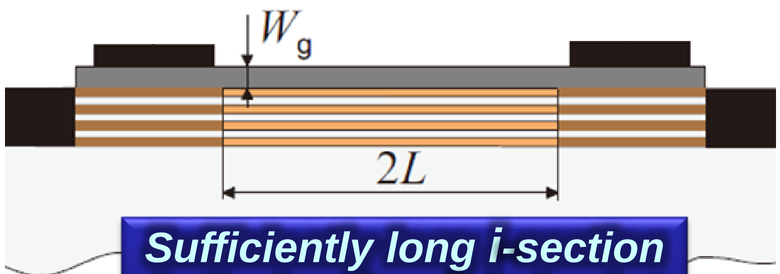

Sufficiently long i-section is the key to minimize I_{tt}!

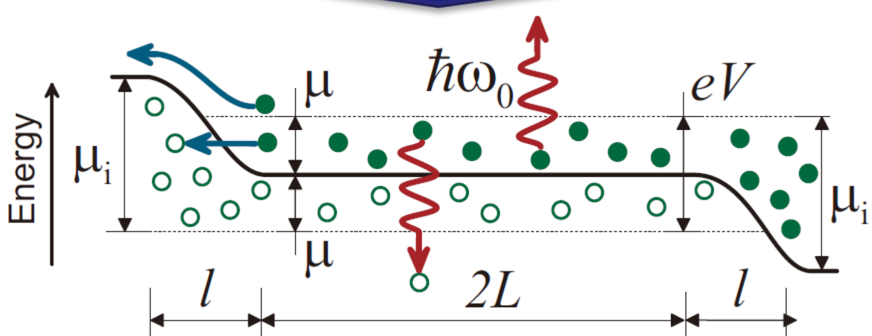

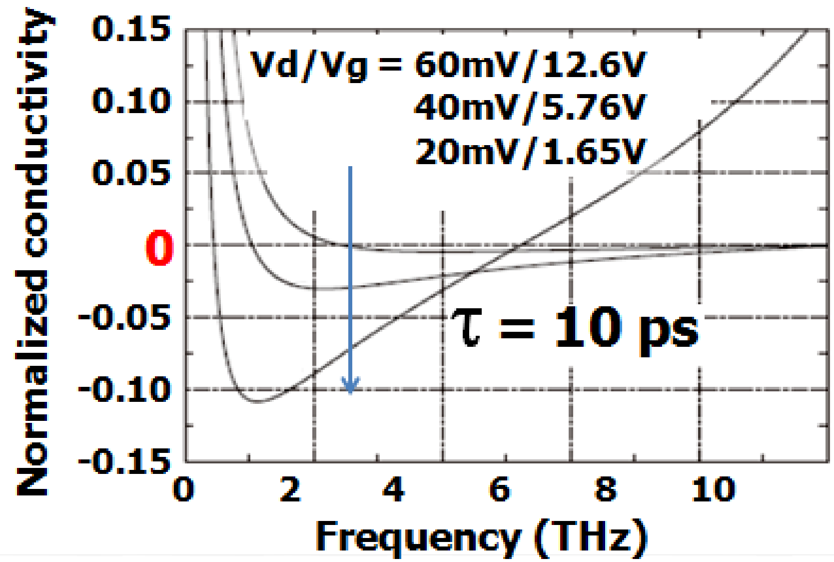

I_{inject} : injection current
I_{tt} : tunneling & thermionic leakage current
η: injection efficiency $= (I_{inject} - I_{tt}) / I_{inject}$
I_{th} : threshold current

Parameters

- $+V_G$ / $-V_G$ $\Rightarrow \eta, I_{th}$
- $V_D \Rightarrow \lambda$ at G_{max}
- $L \Rightarrow \eta > 0$

Benchmarking GRL over QCL & Raman-L

Figure of merits \ Laser type	QCL	Graphene-L		Raman-L
	Injection pump	Injection pump	Optical pump	Optical pump
Mechanism	ISB	IB		SRS
Quantum efficiency	~N of QCs	~ 1		low
Pumping efficiency	high	high	low @IR or moderate @THz (CO_2)	very low
Gain/volume	low	high (large α & emission by plasmon modes)		very low
Freq. range	down to 1.5 THz at lowered temp.	down to 1 THz at elevated temp.		down to 1 THz at elevated temp.
Operating temp.	low	could be high		could be high
Heat spread	×	O		×
Linewidth	very narrow	could be narrow by plasmon instability		narrow
Fabrication	complex SLs with MBE	easy epi with MBE		easy bulky,fiber
Size	compact	compact		large

?

Is it possible to get lasing from graphene?

?

Is it possible to get lasing from graphene?

Yes, optical and injection pumping can be achieved

Outline

- Introduction and Motivation
- Optoelectronic Properties of Graphene
- Optically Pumped THz Lasers
- Current Injection THz Lasers
- *Double Graphene Layer Structures*
- Plasmonic Enhancement
- Summary

Double-GL structures and their features

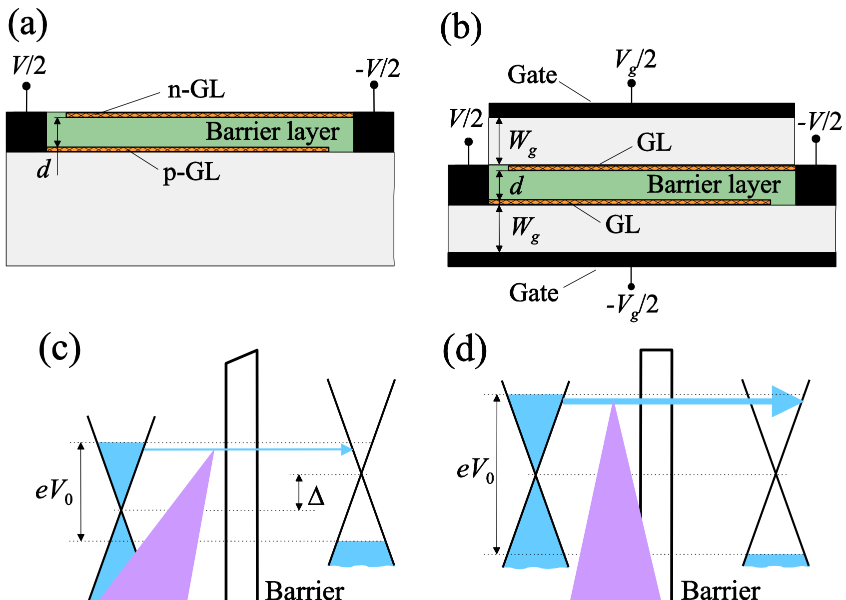

Non-resonant inter-GL tunneling

Resonant inter-GL tunneling

(1) Voltage control of electron and hole densities and interband and intraband absorption of radiation

(2) Inter-GL tunneling, including resonant tunneling, negative differential conductivity

(3) Plasma oscillations in double-GL structures – each GL serves as the gate for another GL!

V. Ryzhii, A. Satou, T. Otsuji, M. Ryzhii, V. Mitin, M. S. Shur, J. Phys. D: Appl. Phys. (2013)

Admittance vs frequency at different quality factors of plasma oscillations

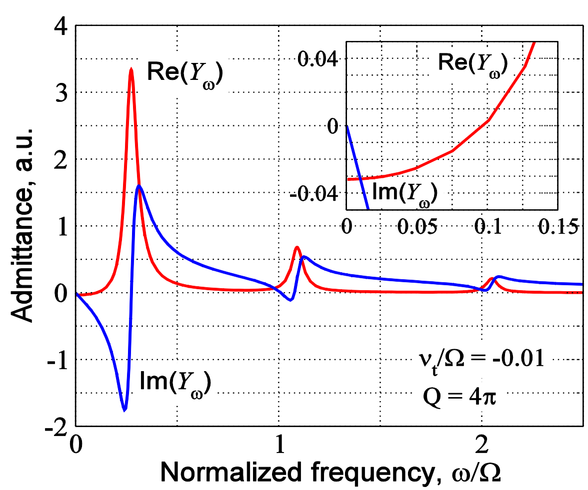

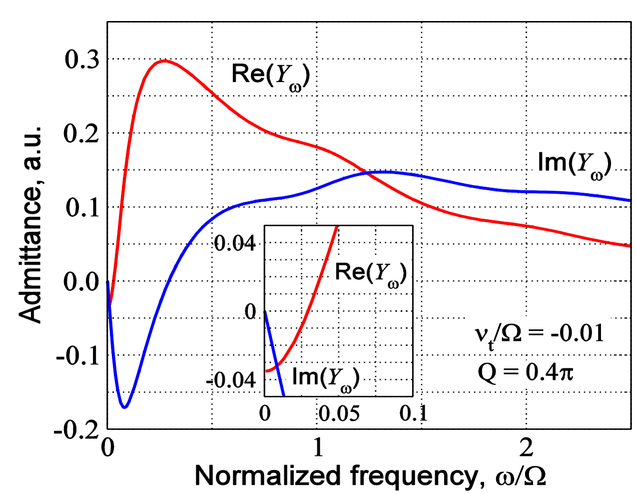

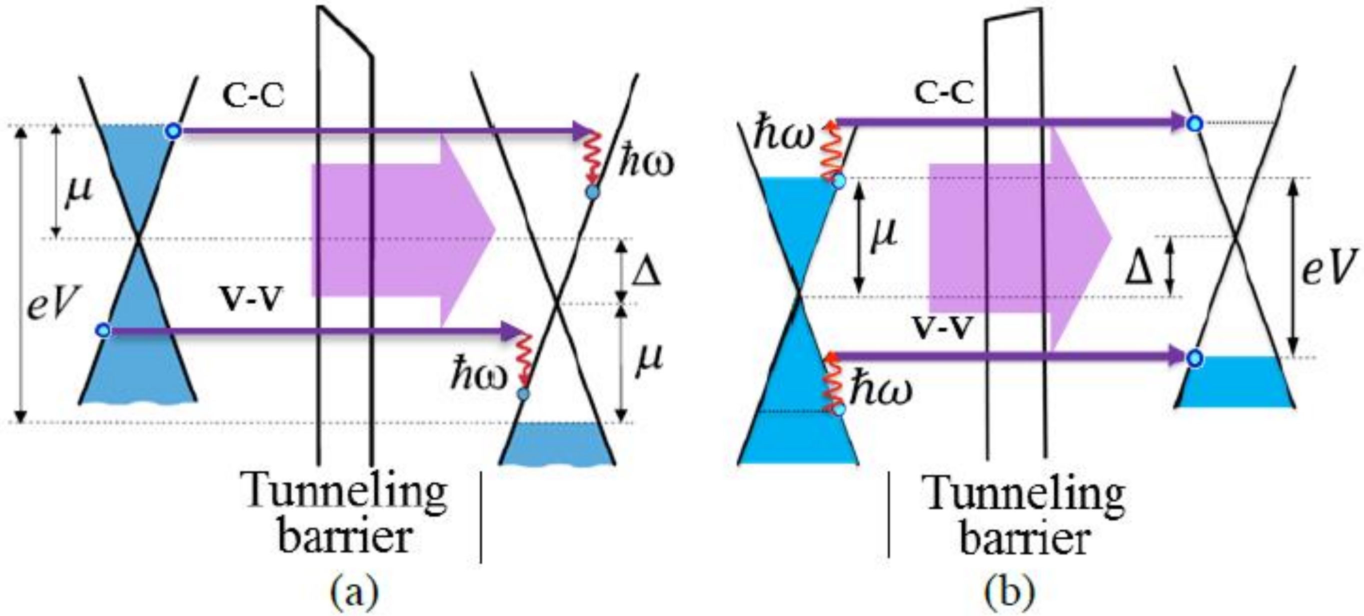

Band diagrams of laser/PD structures with (a) photoemission-assisted inter-GL and (b) photo-absorption-assisted inter-GL radiative transistions

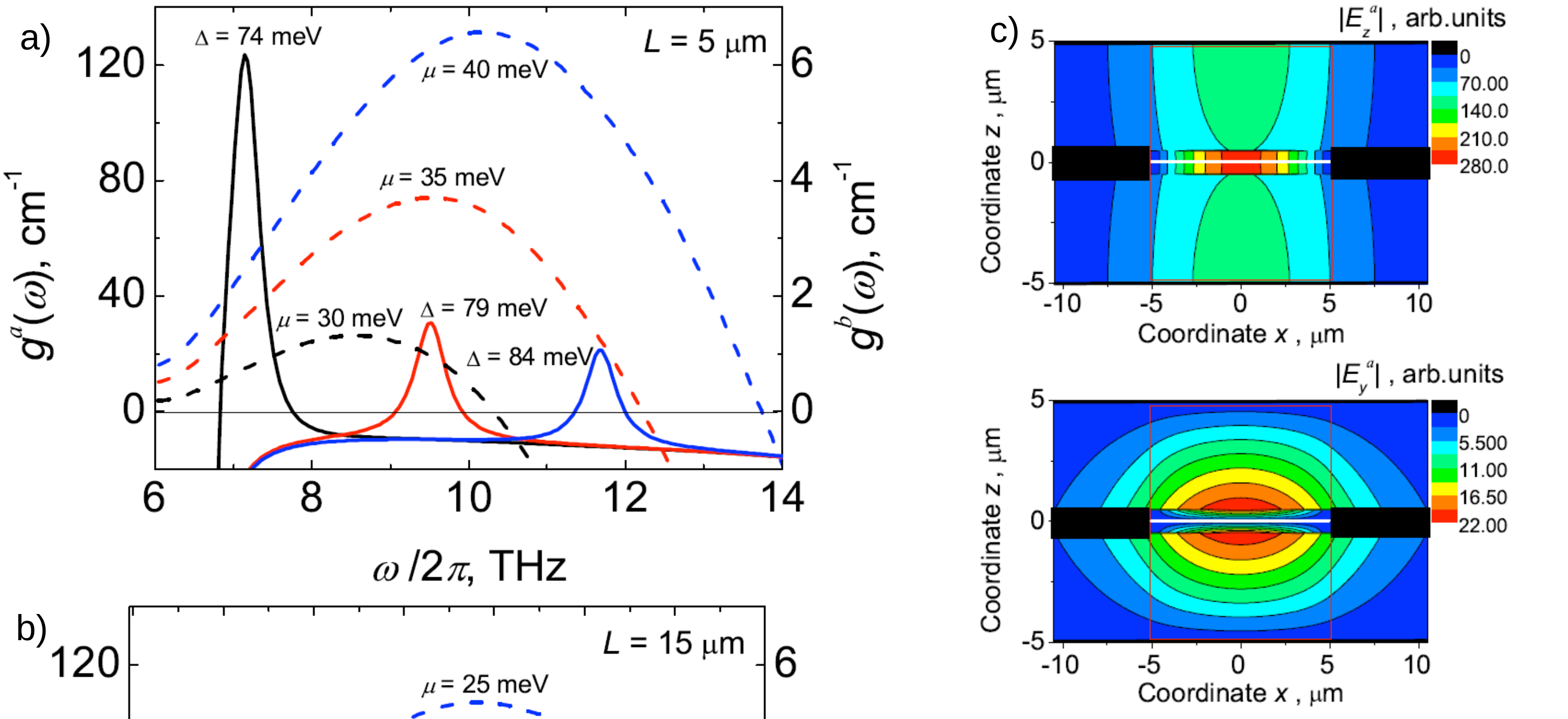

Simulated frequency dependence of the THz gain for the D-GL inter-GL transition laser for different band-offset energies between the Dirac points and of the THz gain for the D-GL intra-GL transition laser for different Fermi energies in GLs: (a) *L* = 5μm and *W* = 5μm, and (b) *L* = 15μm and *W* = 5μm. (c) Simulated spatial distributions of the photon electric field components in the TM mode in the DGL inter-GL transition laser.

?

What is an advantage of a double graphene layer structure?

?

What is an advantage of a double graphene layer structure?

One of advantages is resonant tunneling at a controlled frequency of absorption and/or emission

Outline

- Introduction and Motivation
- Optoelectronic Properties of Graphene
- Optically Pumped THz Lasers
- Current Injection THz Lasers
- Double Graphene Layer Structures
- *Plasmonic Enhancement*
- Summary

TOHOKU UNIVERSITY RIEC

2D Plasmons in Graphene

V. Ryzhii, A. Satou, T. Otsuji, ***JAP* 101**, 024509 (2007).
V. Popov, , T.Y. Bagaeva, T. Otsuji, V. Ryzhii, ***PRB* 81**, 073404 (2010).
V. Ryzhii, M. Ryzhii, V. Mitin, A. Satou, T. Otsuji, ***JJAP* 50**, 094001 (2011).

Normal semiconductors

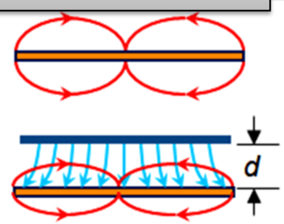

ungated 2D: $\omega = \sqrt{\frac{e^2 n}{2\varepsilon m} k}$

gated 2D: $\omega = \sqrt{\frac{e^2 n d}{\varepsilon m}} \cdot k \propto k d^{1/2} V_g^{1/2}$

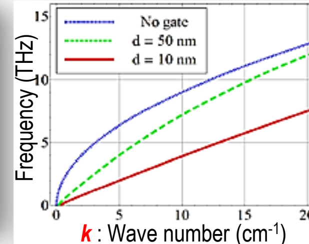

Gated graphene

$(s \gtrsim v_F, \; |k|^{-1} \gg d)$

$$\omega = ks \approx k\sqrt{\frac{4\ln 2 e^2 d k_B T}{\varepsilon \hbar^2}} \propto k d^{1/2} T^{1/2}$$

$$\varepsilon_F = \hbar \upsilon_F \sqrt{\varepsilon V_g / 2ed} \begin{cases} << k_B T \\ >> k_B T \end{cases}$$

$$\omega = ks \approx k\upsilon_F \sqrt{\frac{\alpha}{2}} \propto k \upsilon_F d^{1/4} V_g^{1/4}$$

Gated graphene ribbon array

$$\tilde{\omega}_p = \omega_p - i\gamma = \sqrt{\frac{4\pi e^2 n}{\wp m^*} \frac{q \cos^2\theta}{1 + \coth(qd)} - \frac{1}{4\tau^2}} - i\frac{1}{2\tau}$$

e : elementary charge, $\wp$: the permittivity
d : the period of the GRA
τ : the momentum relaxation time of electrons

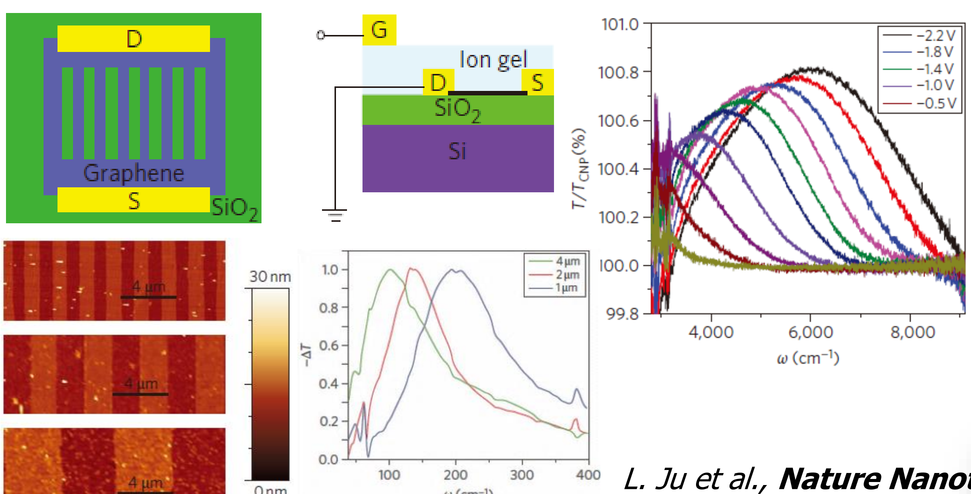

L. Ju et al., ***Nature Nanotech.* 6**, 630 (2011).

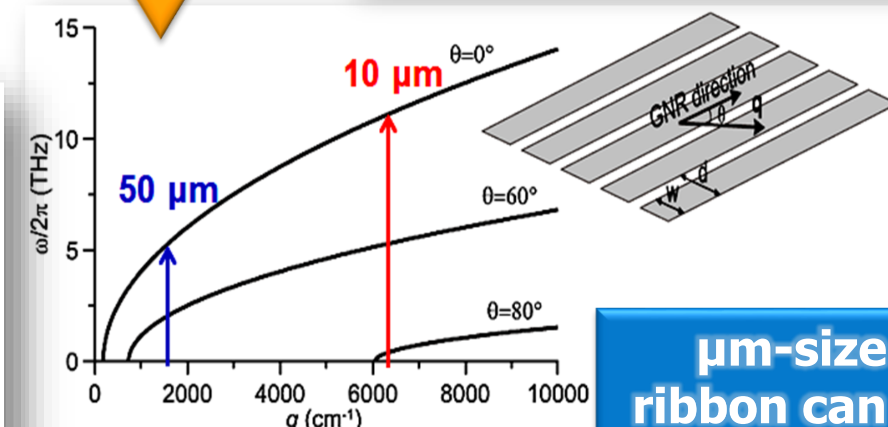

μm-size ribbon can resonate in THz

Plasma oscillations: spatial distributions of ac potentials in GLs

Plasma oscillations in double-GL structures – each GL serves as the gate for another GL!

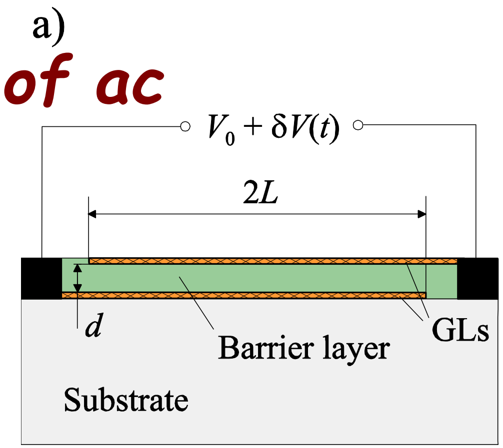

$$\delta\varphi_+ = \frac{\delta V_m}{2}\left(\frac{\cos(\gamma_\omega x)}{\gamma_\omega \sin(\gamma_\omega L)} - x\right)\Big/\left(\frac{\cos(\gamma_\omega L)}{\gamma_\omega \sin(\gamma_\omega L)} - L\right)$$

$$\delta\varphi_- = -\frac{\delta V_m}{2}\left(\frac{\cos(\gamma_\omega x)}{\gamma_\omega \sin(\gamma_\omega L)} + x\right)\Big/\left(\frac{\cos(\gamma_\omega L)}{\gamma_\omega \sin(\gamma_\omega L)} - L\right)$$

$$\gamma_\omega = \sqrt{2\omega(\omega + i\nu)}\,/\,s$$

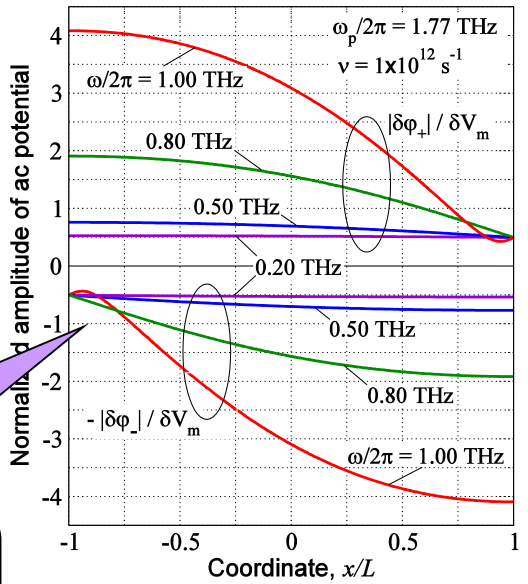

Excitation of standing plasma waves in double-GL structures – resonantly high voltage amplitudes

V. Ryzhii, T. Otsuji, M. Ryzhii, V. Leiman, S. O. Yurchenko, V. Mitin, M. S. Shur, J. Appl. Phys. **112,** 104507 (2012)

Responsivity vs signal frequency at different plasma and collision frequencies

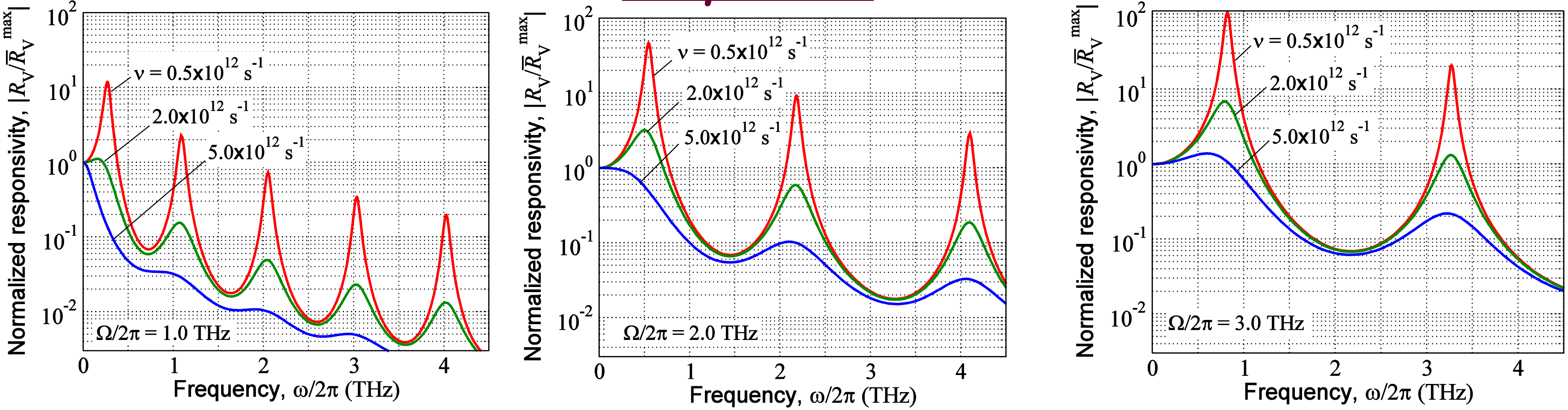

V_0 = 0.5 V, R_V = 10^4 - 10^5 V/W

Dependence of normalized responsivity $R_V/\overline{R}_V$ versus bias voltage swing $(V_0 - V_t)/\Delta V_t$.n at different signal frequency ω near the zeroth plasma resonance (upper panel) and near the first plasma resonance (lower panel).

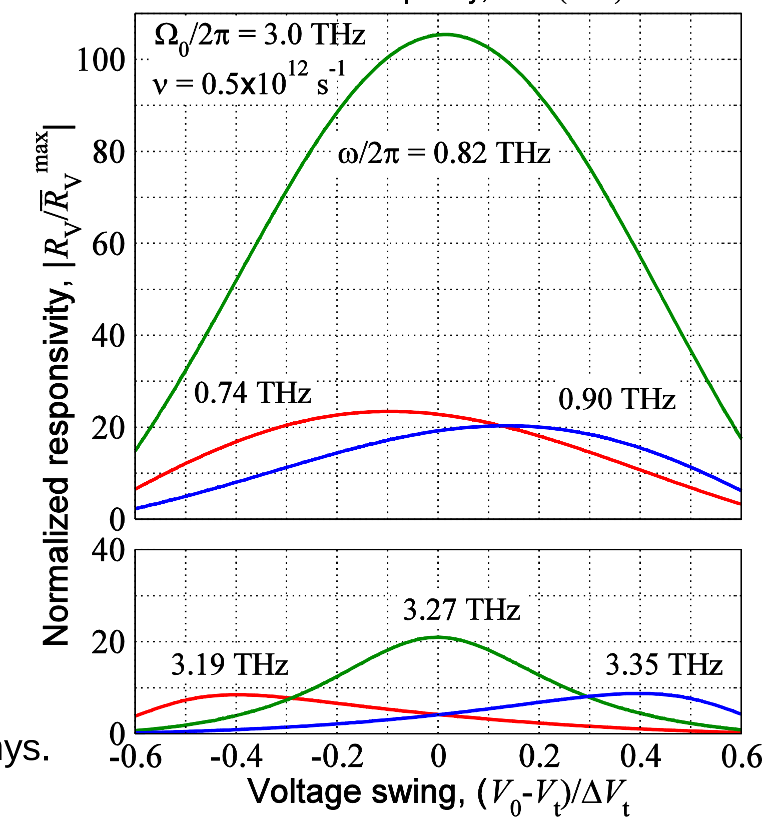

V. Ryzhii, T. Otsujj, M. Ryzhii, and M. S. Shur, J. Phys. D: Appl. Phys. (2012)

V. Ryzhii, A. Satou, T. Otsuji, M. Ryzhii, V. Mitin, M. S. Shur, J. Phys. D: Appl. Phys. (2013)

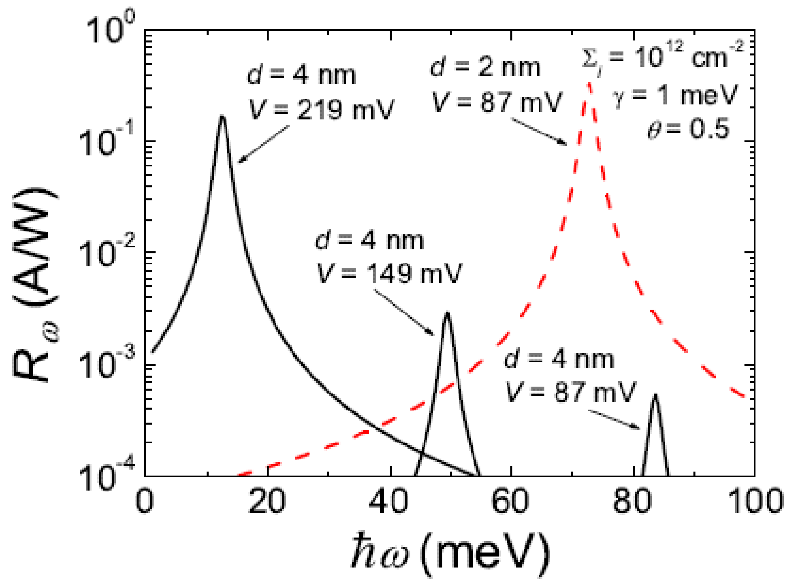

$$R_\omega = \left(\frac{\pi e^2}{c\hbar}\right)\frac{8e|z_{u,l}|^2\gamma}{[\hbar^2(\omega-\omega_{max})^2+\gamma^2]}\left(\Sigma_i + \frac{\kappa\Delta}{4\pi e^2 d}\right)\theta$$

$$\frac{\Delta}{e} = V + V_0 - \sqrt{2VV_0 + V_0^2 + V_t^2}$$

$$\hbar\omega \simeq -\Delta + \hbar\omega_{dep} = \hbar\omega_{max}$$

The DLG-PD responsivity R_ω versus the photon energy $\hbar\omega$ calculated for different voltages V

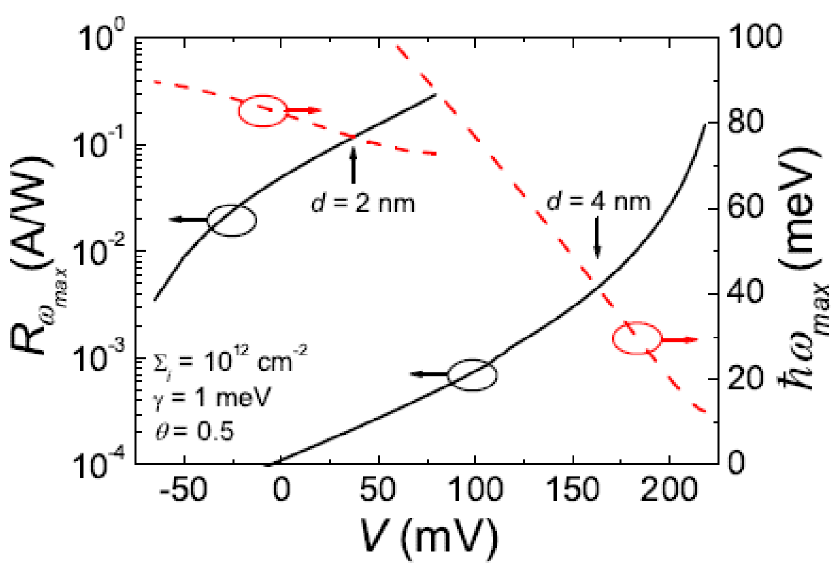

$$R_{\omega_{max}} = \left(\frac{e\kappa\, d}{c\hbar}\right)\left(\frac{\hbar\omega_{dep}}{\gamma}\right)\theta$$

This shows the dependencies of photon energy $\hbar\omega_{max}$ and responsivity maximum $R_{\omega max}$ on the applied voltage V calculated for different thicknesses of the inter-GL barrier layer d. A marked shift in the responsivity maxima with varying bias voltage enables the DGL-PD spectrum voltage tuning.

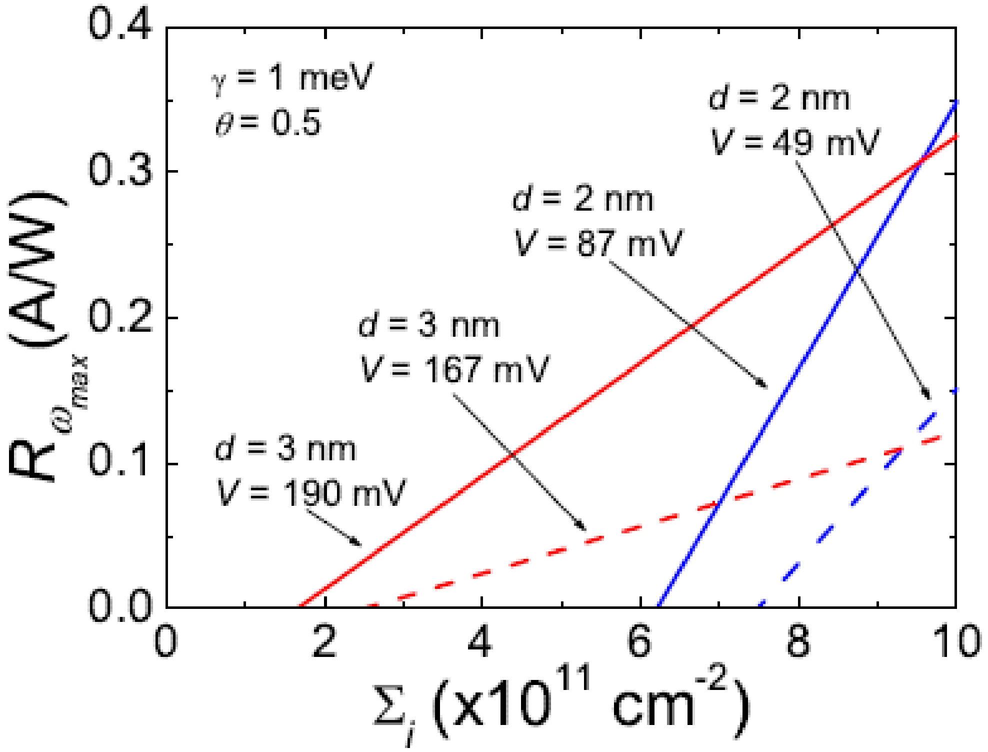

$$\Sigma_i \propto V_g / W_g$$

This shows the dependency of the responsivity maximum $R_{\omega max}$ on the electron and hole density Σ_i and different bias voltages V and thicknesses d. The maximum of the DGL-PD responsivity markedly depends on electrical doping determined by the gate voltage V_g

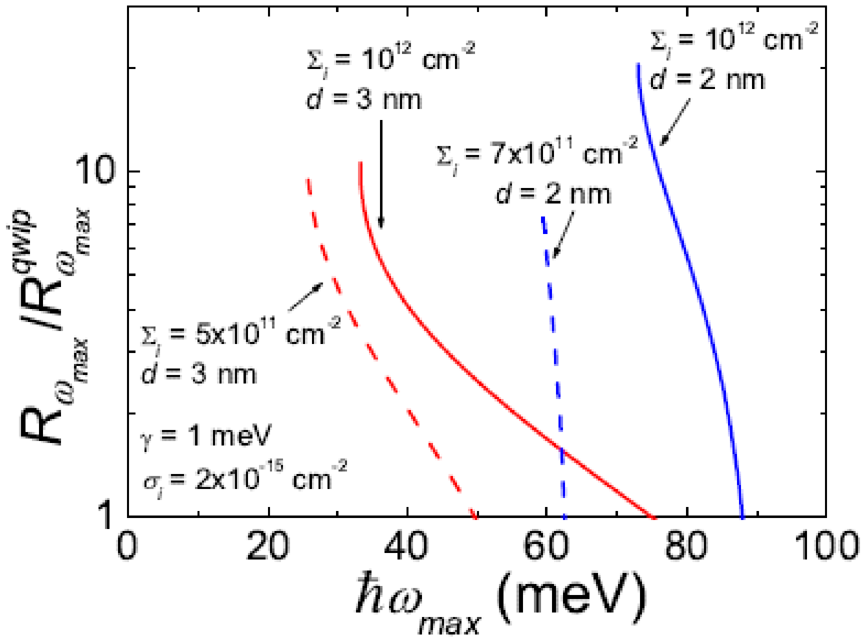

$$R_\omega^{pin} \simeq \left(\frac{\pi e^2}{c\hbar}\right)\frac{eg^{pin}}{\hbar\omega}, \; R_\omega^{qwip} \simeq \left(\frac{e}{\hbar\omega}\right)\sigma_i\Sigma_i\, g^{qwip}\theta$$

$$\frac{R_{\omega_{max}}}{R^{pin}_{\omega_{max}}} \simeq \frac{\hbar^2\omega_{max}\omega_{dep}\theta}{\varepsilon_d\gamma\, g^{pin}}, \quad \frac{R_{\omega_{max}}}{R^{qwip}_{\omega_{max}}} \simeq \frac{\hbar^2\omega_{max}\omega_{dep}}{\varepsilon_i\gamma\, g^{qwip}}$$

$$\varepsilon_d = 2\pi e^2/\kappa\, d \qquad \varepsilon_i = c\hbar\sigma_i\Sigma_i/\kappa\, d$$

This shows the ratios of DGL-PD and QWIP responsivity versus photon energy $\hbar\omega_{max}$ for different electron and hole densities Σ_i and thicknesses of the inter-GL barrier layer, *d*

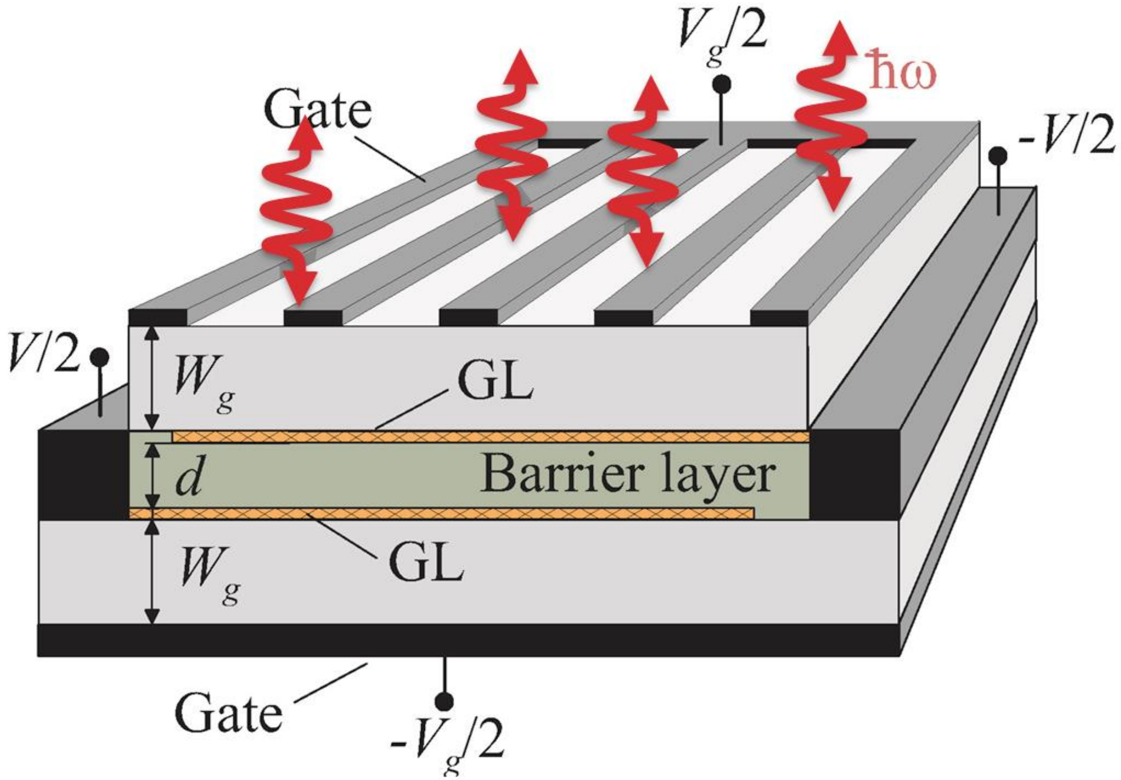

A graphene plasmonic heterostructure for THz lasers and detection

Enhanced THz Responsibities via PA-RT & Plasmon Resonances in DGLs

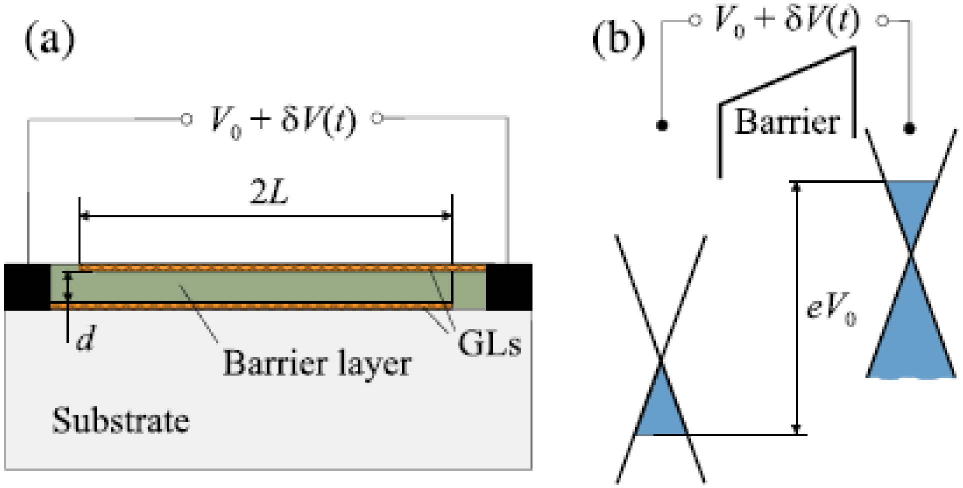

V. Ryzhii et al., ***APL 104***, *163505 (2014).*
V. Ryzhii et al., ***J. Phys. D 45***, *302001 (2012).*

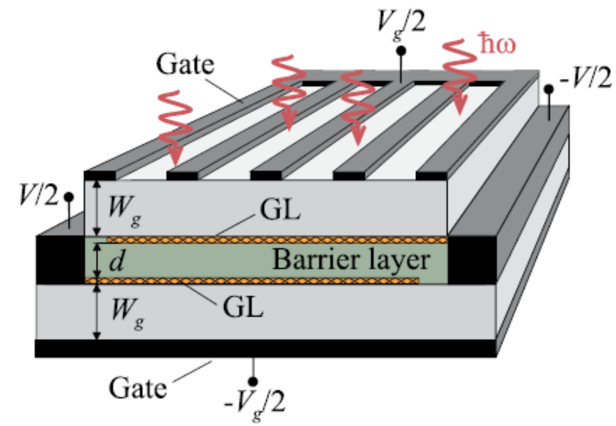

Resonant THz Detections via GR-SPPs

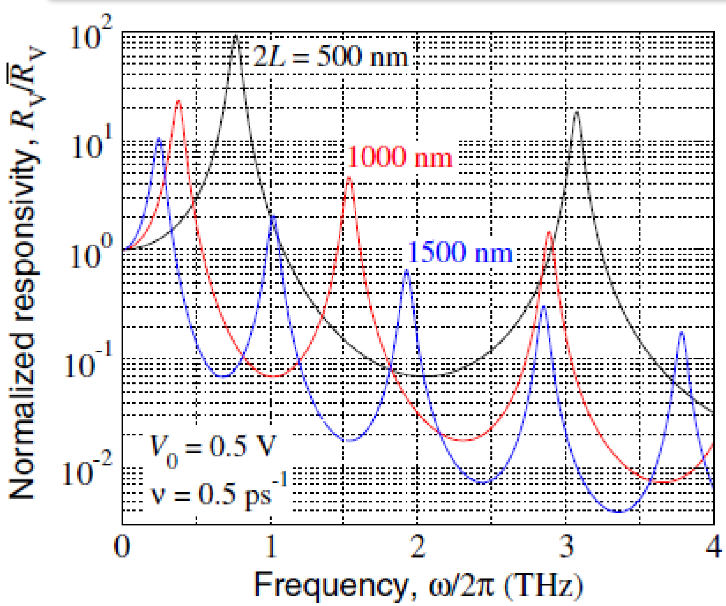

Resonant THz Detections via PA-RT

PA-RT: Photon-Assisted Resonant Tunneling

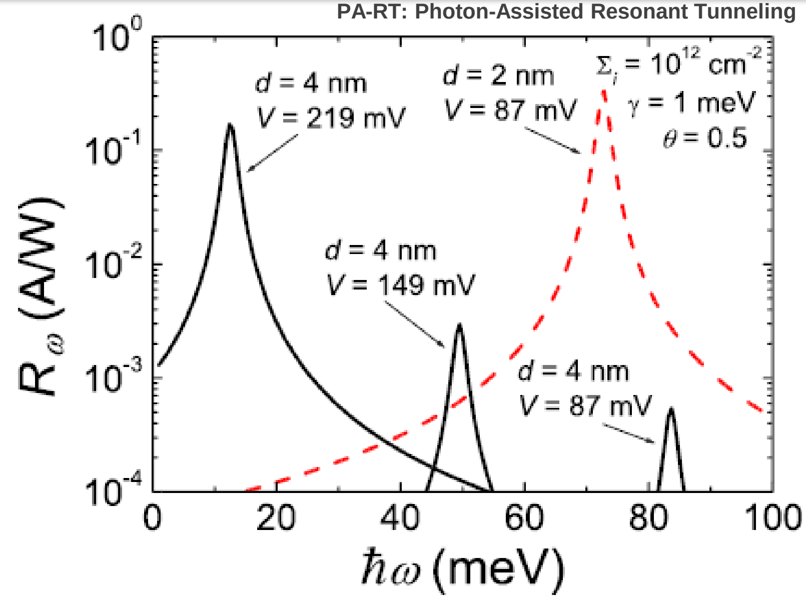

Observed THz Gain Exceeding the $e^2/4\hbar$ Limit by Orders

S. Boubanga Tombet et al., ***PRB 85*** *, 035443 (2012).*

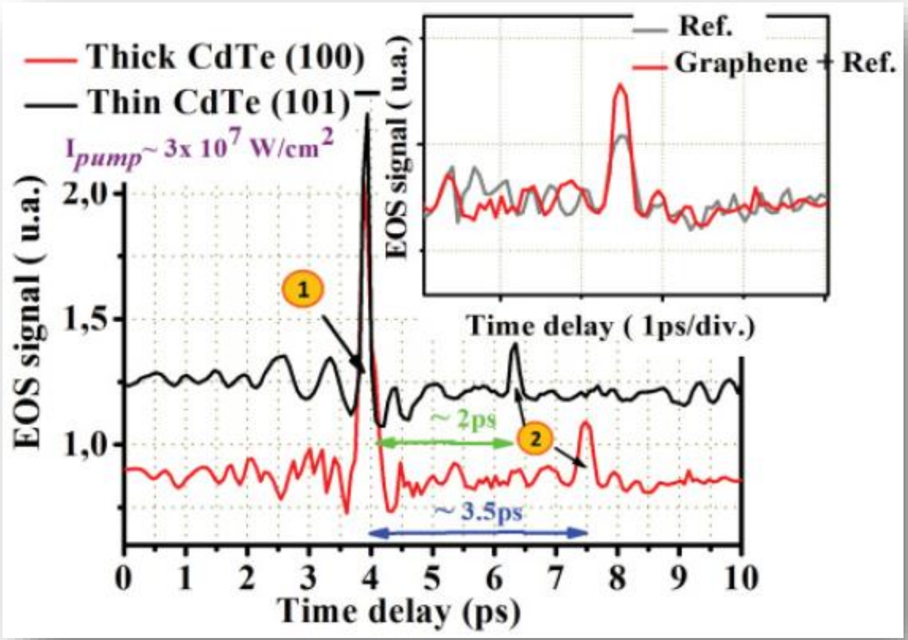

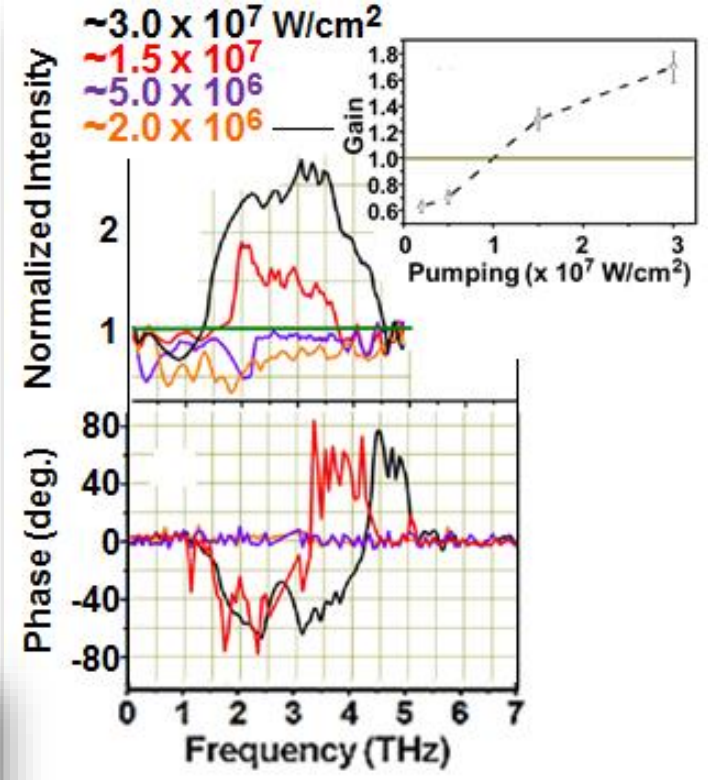

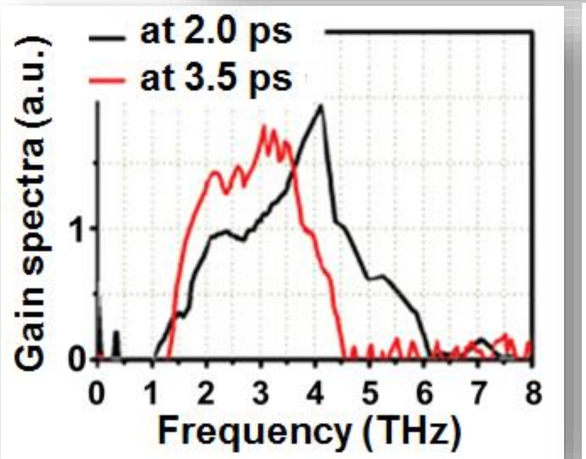

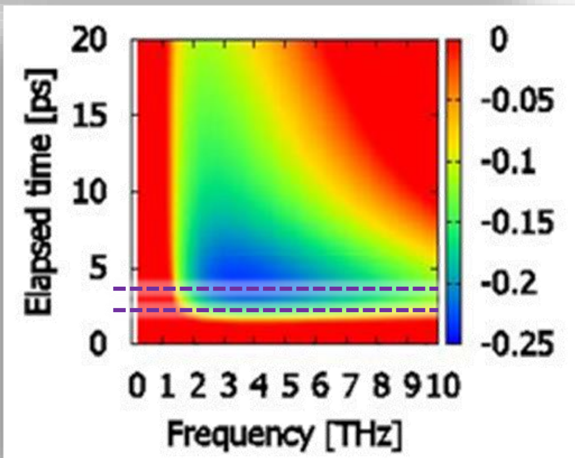

?

Do plasmonics add frequency selectivity?

?

Do plasmonics add frequency selectivity?

2D plasmons in graphene enhance the light-matter interaction.

Summary

Concepts of THz & IR devices based on graphene structures were reviewed.

Optically pumped graphene can generate in a wide THz range.

Current injection G-Lasers, implementing in dual gate G-FETs, have a great advantage to dramatically decrease the equivalent pumping photon energy, resulting in NDC at rather low injection currents.

Double graphene layer structure is a promising engineered material.

2D plasmons in graphene enhance the light-matter interaction.

As preliminary experimental results ehow, the presented devices are realistic: they can exhibit very high performance


Thank You

Introduction:

Population Inversion in Optically Pumped Graphene
– Original Idea for GR-THz Lasers

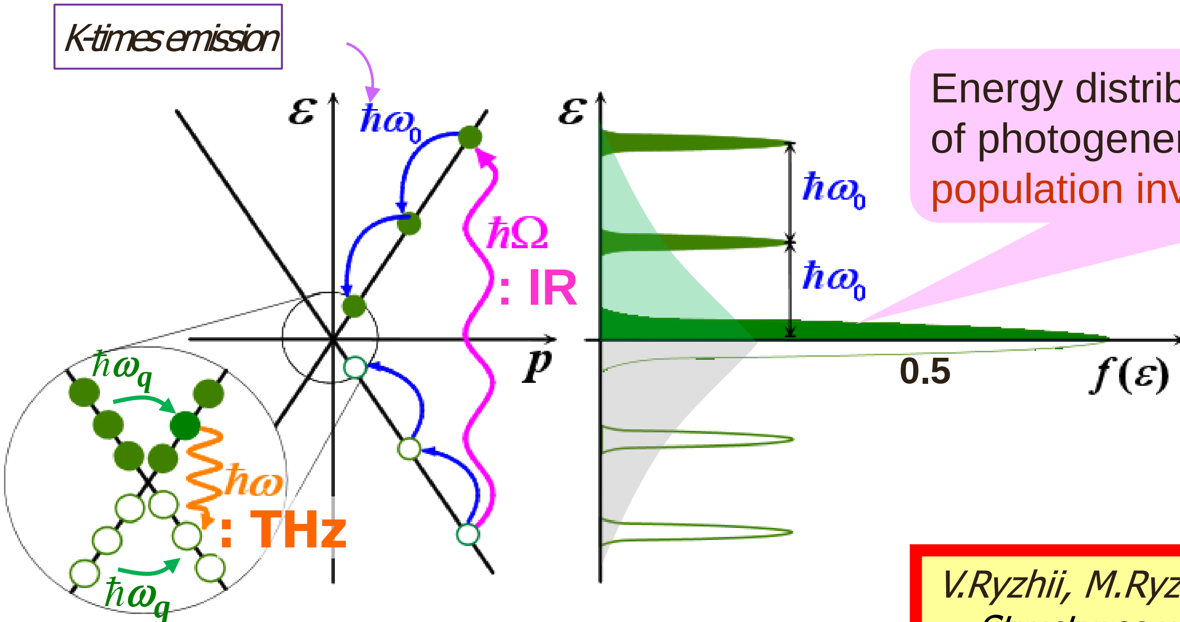

Energy distributions
of photogenerated electrons and holes –
population inversion

V.Ryzhii, M.Ryzhii, T.Otsuji, JAP **101**, *083114 (2007): Structures with negative dynamic conductivity in resonant cavity can be used as THz emitters*

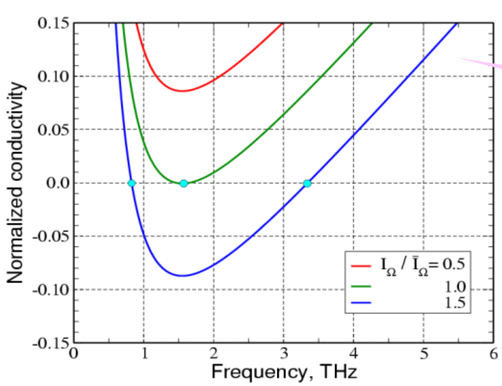

Range of negative dynamic conductivity (at sufficiently strong optical pumping) –
Interband transitions vs intraband (Drude absorption)

Population Inversion of *e-h* Pairs, Negative Absorption, and Lasing

Limitations of continuous scheme (heating by optical phonons, non-radiative recombination, etc.) may be resolved under transient regime of pumping

Model for transient regime of lasing

- Population inversion with quasi-Fermi energy ε_F takes place during $t_{p-eq} < t < t_{rec}$, where t_{p-eq}~ duration of pumping and subsequent emission of optical phonons
- Unstable mode with population $N_{\omega t}$ ~exp(t/t_{rad}) propagates along resonator of length L during time ~ t_{rad}
- Minimal length $L > c/\sqrt{\kappa t_{rad}}$
- If t_{rad} ~ 10 ps (see below), one obtains $L > 0.5$ mm
- Output power ~10 - 100 pW per pulse because an active volume is very small

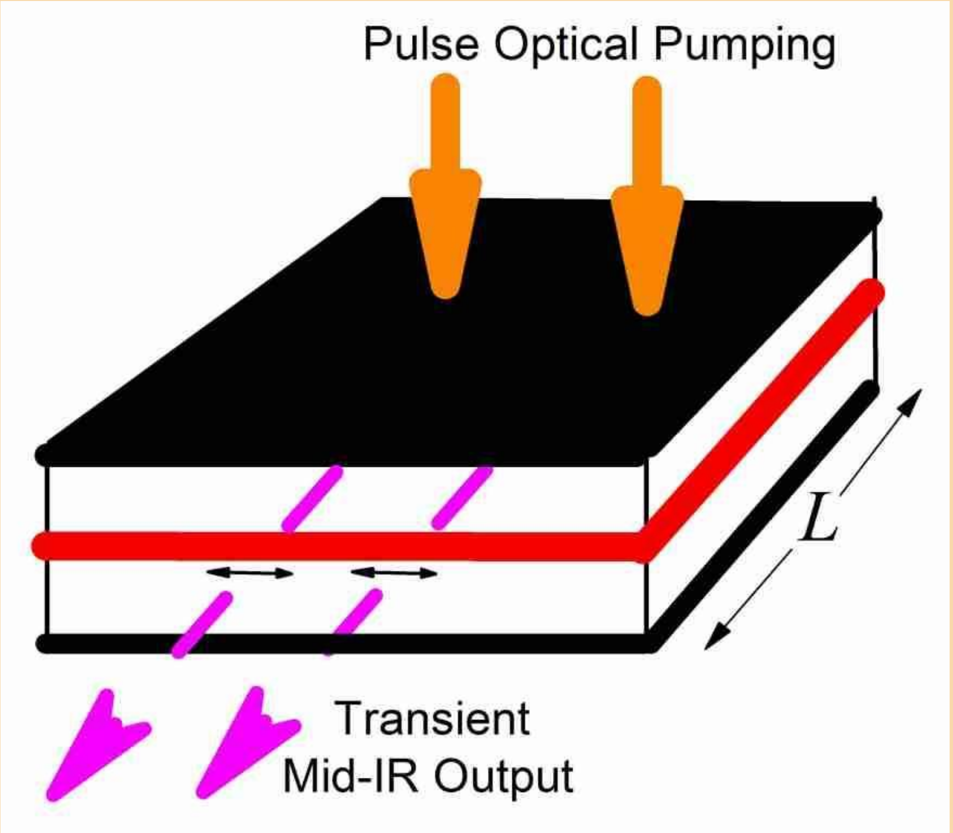

Sketch of graphene (red) in resonator under pulse optical pumping with mid-IR output

<u>Introduction:</u> Femtosecond Population Inversion in Heavily-Doped Graphene

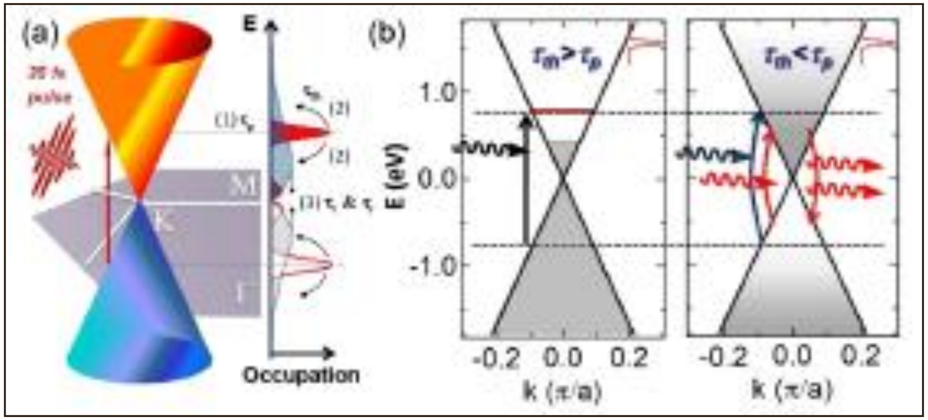

(a) Schematics of ultrafast optical interband excitations.
(b) Dispersion of our electron-doped graphene, monolayers (μ=0.4 eV) illustrating state filling (left) and band filling (right) that leads to stimulated emission from a broadband, inverted population (red arrow). Also shown together is the pump pulse spectrum.

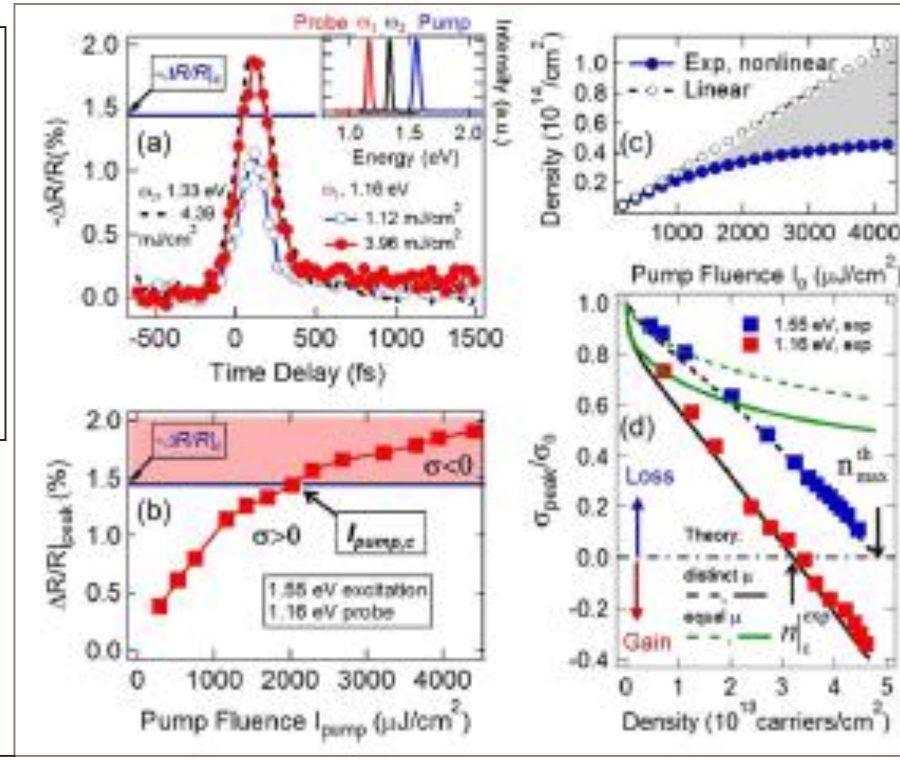

(a) Ultrafast *ΔR/R* at 1.55 eV pump, 1.16 eV probe, at 1116 and 3960 μJ/cm^2, and 1.33 eV probe, at 4390 μJ/cm^2, respectively. Blue arrow marks $\Delta R/R|_c$=-1.4582% for zero conductivity. Shown together are the pump and probe spectra. **(b)** The peak transient reflectivity as function of the pump fluence. **(c)** The extracted transient fermion density at 40 fs (blue dots), as explained in the text, which is significantly lower than $A_0 I_p = \hbar\omega$ obtained from the universal conductivity (open circles), as illustrated in shadow area. **(d)** Theory (lines) vs experimental values (rectangles) for nondegenerate (red) and degenerate (blue) transient conductivity at 40 fs. Shown together (lines) are two model simulations with the single (green) or distinct (black) chemical potentials. **[Phys. Rev. Lett. 108, 167401 (2012)]**

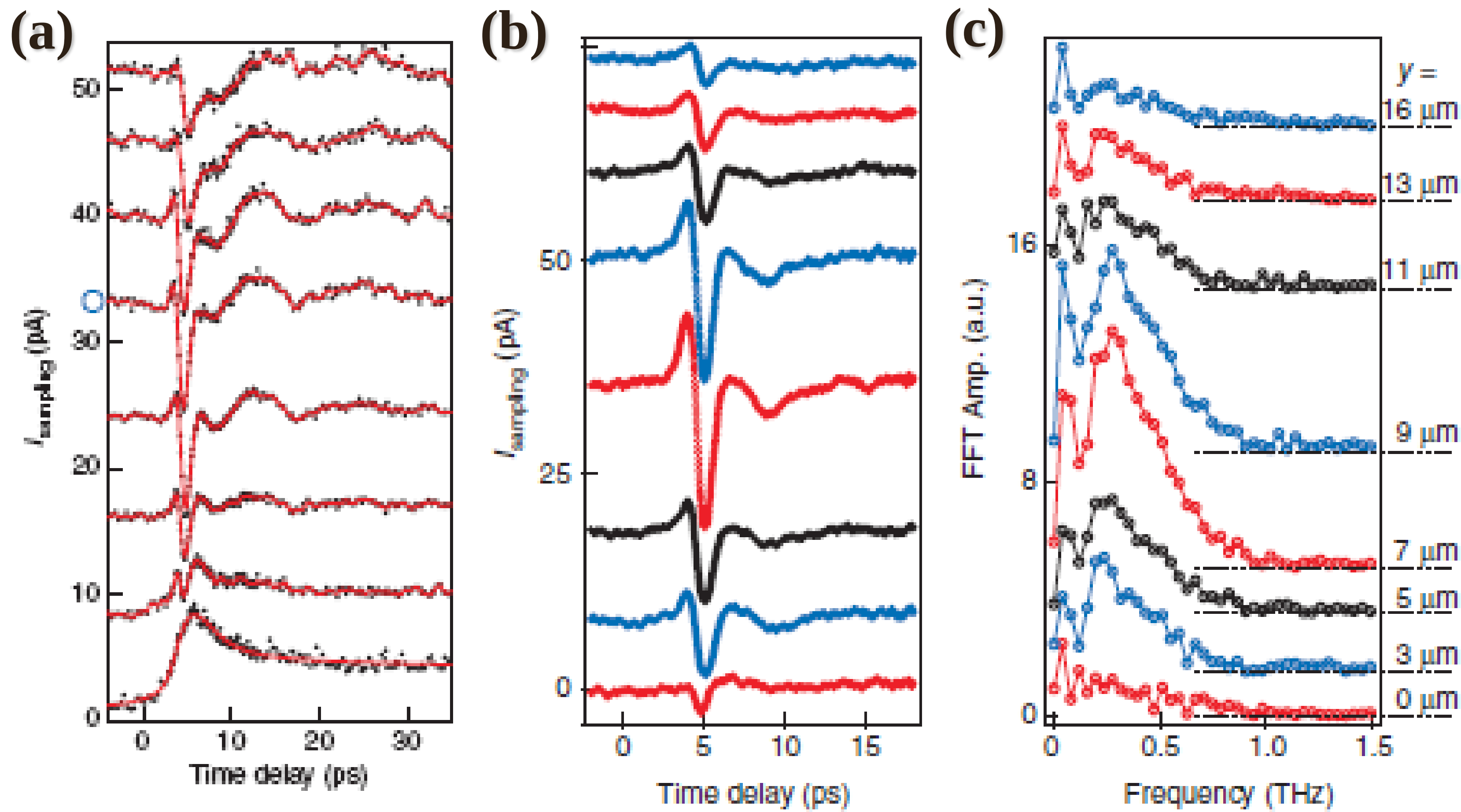

(**a**) $I_{sampling}$ for excitation positions starting at the graphene–metal interface in steps of 2 µm (from bottom to top) along the dotted line in Fig. b. Data are offset for clarity. The parameters are E_{laser} = 1.59 eV, P_{laser} = 800 µW, V_{sd} = 0 V, and T = 300 K.

(**b**) Time-resolved $I_{sampling}$ at T = 77 K for the same parameters as in (a). The position *y* (right) refers to the dotted line in Fig. b.

(**c**) Corresponding fast-Fourier-transformation of $I_{sampling}$ as displayed in (**a**).

Introduction: Time-resolved photocurrents and THz generation in suspended graphene

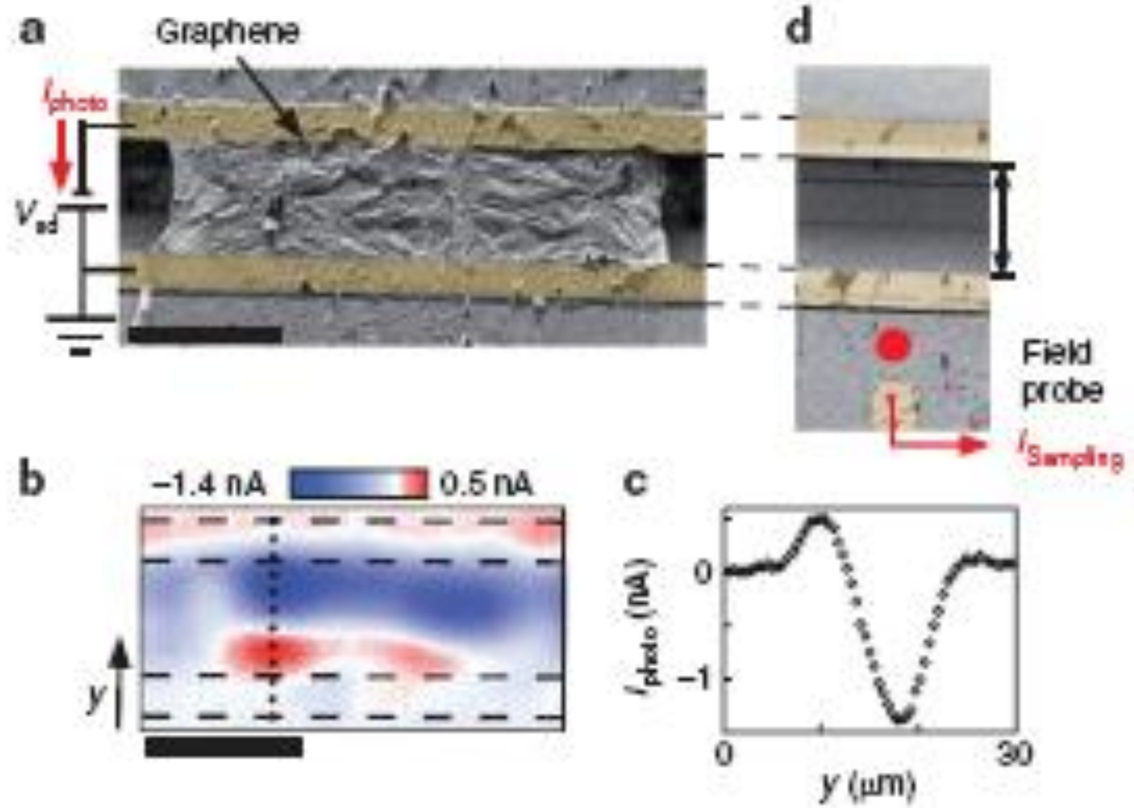

(a) Suspended graphene onto a coplanar stripline circuit. A pump laser pulse focused onto the graphene-sheet generates the time-integrated photocurrent I_{photo}. Scale bar, 20 µm.
(**b**) Spatially resolved scan of I_{photo}. Parameters are E_{laser} = 1.6 eV, P_{laser} = 200 µW, V_{sd} = 0 V.
(**c**) Single line-sweep of I_{photo} along the dotted line in (**b**).
(**d**) The time-resolved photocurrent response $I_{sampling}$ is measured at the field probe, located ~0.3 mm away from the graphene. The probe laser pulse (red circle) triggers the read-out of $I_{sampling}$. All measurements at T=300 K (Nature Comm. **3**, 646, 2012)

Photon-Assisted Resonant Tunneling Enabling Novel THz Functionalities

J. Phys. D: Appl. Phys. 45 (2012) 302001 (6pp) doi:10.1088/0022-3727/45/30/302001

INVITED FAST TRACK COMMUNICATION

Double graphene-layer plasma resonances terahertz detector

V Ryzhii[1,3], T Otsuji[1,3], M Ryzhii[2,3] and M S Shur[4]

J. Phys. D: Appl. Phys. 46 (2013) 315107 (6pp) doi:10.1088/0022-3727/46/31/315107

Dynamic effects in double graphene-layer structures with inter-layer resonant-tunnelling negative conductivity

V Ryzhii[1,3], A Satou[1,3], T Otsuji[1,3], M Ryzhii[2,3], V Mitin[4] and M S Shur[5]

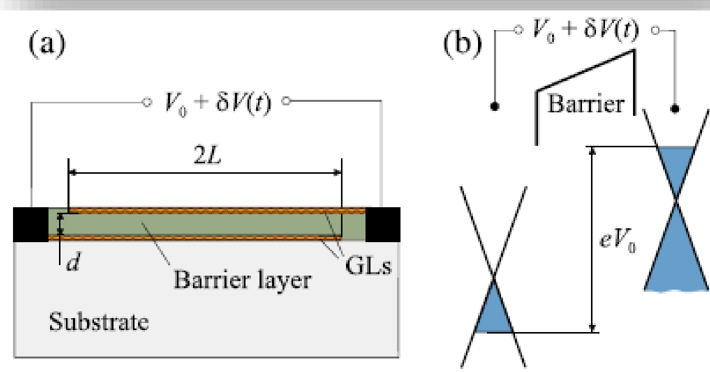

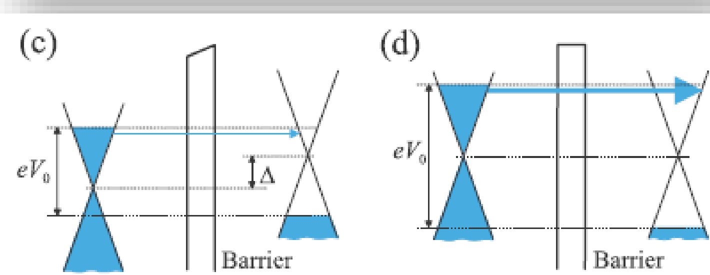

JOURNAL OF APPLIED PHYSICS 113, 174506 (2013)

Terahertz photomixing using plasma resonances in double-graphene layer structures

V. Ryzhii,[1,a)] M. Ryzhii,[2] V. Mitin,[3] M. S. Shur,[4] A. Satou,[1] and T. Otsuji[1]

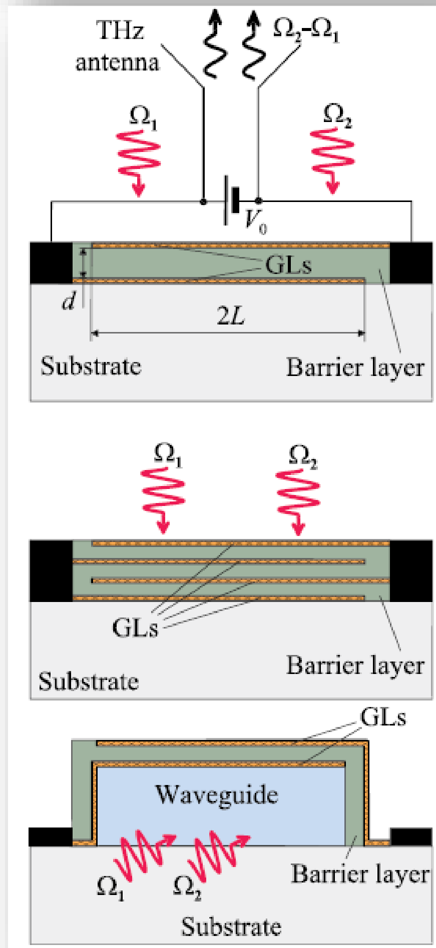

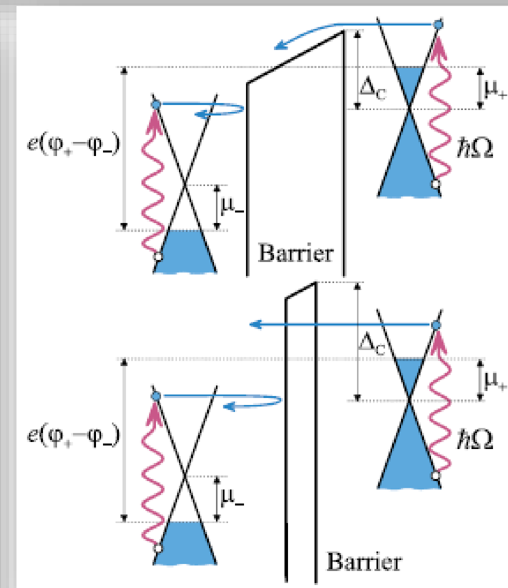

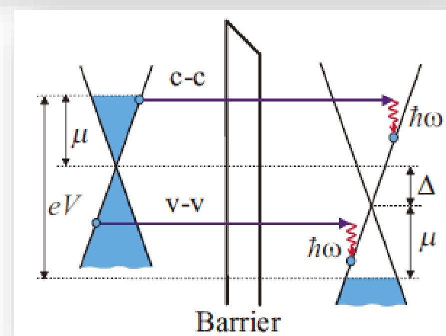

Double-GL structures resonant tunneling

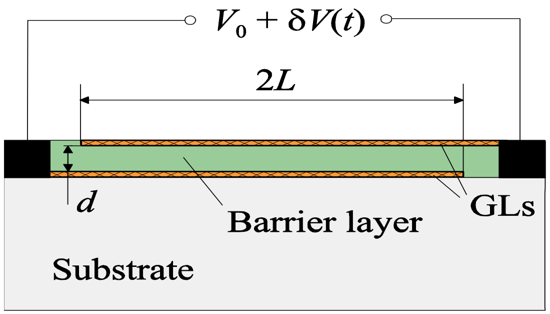

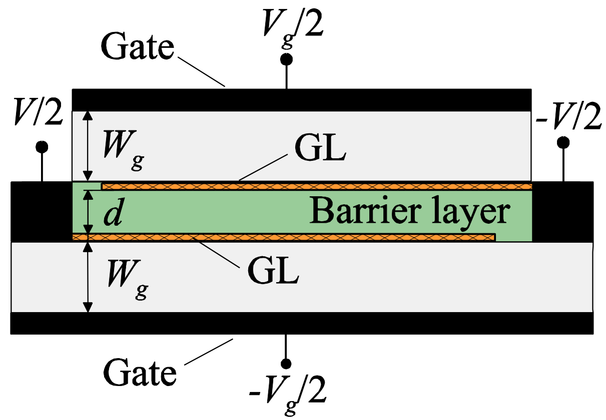

Operation principle:
-THz input signals result in inter-GL nonlinear tunneling or thermionic current
-Rectified component of this current – output signal
-Excitation of plasma oscillations leads to resonant increase in inter-GL current and output signal

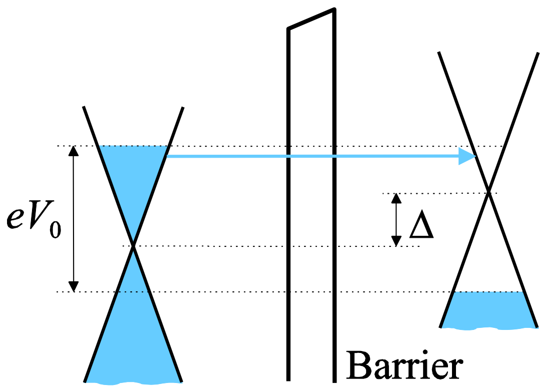

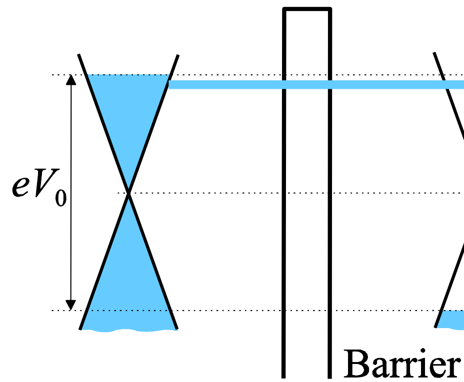

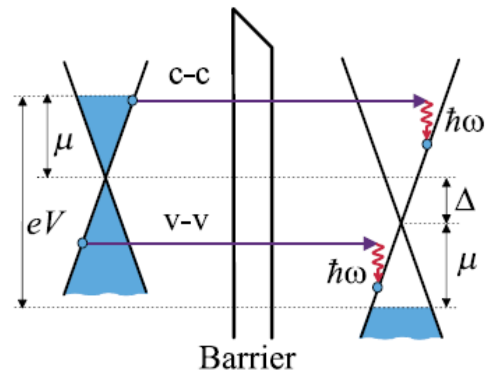

Resonant inter-GL tunneling promotes high detector responsivity!!!

Each GL serves as a gate for another GL!!!

V. Ryzhii, T. Otsuji, M. Ryzhii, V. Mitin and M. S. Shur, J. Phys. D: Appl. Phys. (2012)
V. Ryzhii, A. Satou, T. Otsuji, M. Ryzhii, V. Mitin, M. S. Shur, J. Phys. D: Appl. Phys. (2013)